Ye *et al. J Mater Inf* 2023;3:15
DOI: 10.20517/jmi.2023.08

Journal of Materials Informatics

Research Article

Open Access

Assessment of phase equilibria and thermodynamic properties in the Fe-RE (RE = rare earth metals) binary systems

Hongjian Ye[1], Maohua Rong[1,2,*], Qing Chen[3], Qingrong Yao[1], Jiang Wang[1,2,*], Guanghui Rao[1,2], Huaiying Zhou[1,2]

[1]School of Materials Science and Engineering & Guangxi Key Laboratory of Information Materials, Guilin University of Electronic Technology, Guilin 541004, Guangxi, China.
[2]Engineering Research Center of Electronic Information Materials and Devices, Ministry of Education, Guilin University of Electronic Technology, Guilin, Guangxi, China.
[3]Thermo-Calc Software AB, Solna SE-16967, Sweden.

[*]**Correspondence to:** Dr. Maohua Rong, Prof. Jiang Wang, School of Materials Science and Engineering & Guangxi Key Laboratory of Information Materials, Guilin University of Electronic Technology, Jinji Road No. 1, Guilin 541004, Guangxi, China. E-mail: rongmh124@guet.edu.cn; waj124@guet.edu.cn

How to cite this article: Ye H, Rong M, Chen Q, Yao Q, Wang J, Rao G, Zhou H. Assessment of phase equilibria and thermodynamic properties in the Fe-RE (RE = rare earth metals) binary systems. *J Mater Inf* 2023;3:15. https://dx.doi.org/10.20517/jmi.2023.08

Received: 1 Mar 2023 **First Decision:** 15 May 2023 **Revised:** 3 Jun 2023 **Accepted:** 14 Jun 2023 **Published:** 12 Jul 2023

Academic Editors: William Yi Wang, Xingjun Liu **Copy Editor:** Dong-Li Li **Production Editor:** Dong-Li Li

Abstract

This study focuses on investigating phase equilibria and thermodynamic stability of intermetallic compounds made of the transition metal Fe and rare earth (RE) elements. By using the CALPHAD method and reliable experimental information from the literature, the binary systems of Fe-Y, Fe-Er, and Fe-Lu were reassessed. To improve our previous calculations of Fe-RE (RE = Tb and Dy) binary systems, the Gibbs energy expressions of intermetallic compounds Fe_2Tb and Fe_2Dy were modified to avoid artificial breaks in their heat capacity curves. Thermodynamic parameters obtained are self-consistent, and the Gibbs energies of the Fe-RE (RE = Tb, Dy, Er, Lu, and Y) phases were accurately expressed to reappear available both thermodynamic data and phase equilibria. This work was further combined with the previous calculations of the Fe-RE (RE = La, Ce, Pr, Nd, Sm, Gd, Ho, and Tm) systems to discuss thermodynamic characteristics and phase equilibria of Fe-RE binary systems in detail. A trend was noticed for the change of thermodynamic properties and phase equilibria of the Fe-RE binary systems with RE atomic number. Generally, as the RE atomic number increases, the formation temperatures of the Fe-RE intermetallic compounds increase gradually, and the enthalpy of mixing of liquid Fe-RE (apart from Fe-Y and Fe-Ce) alloys and

the enthalpy of formation of the Fe-RE (apart from Fe-Y, Fe-Ce, Fe-Gd, and Fe-Dy) intermetallic compounds become increasingly negative. The results provide a thorough set of thermodynamic parameters of thirteen Fe-RE binary systems, which could serve as a sound basis for developing a thermodynamic database of Fe-RE-based alloy systems.

Keywords: Fe-RE binary systems, Phase equilibria, Thermodynamic

INTRODUCTION

The intermetallic compounds made of the transition metal Fe and rare earth (RE) elements have been studied extensively because of their excellent physical properties[1-3]. For example, $Fe_{17}RE_2$ compounds exhibit large negative thermal expansion below the Curie temperature, which has numerous high-precision technology and positioning instrument applications[4-6]. Fe_2RE compounds, such as Terfenol-D plates (i.e., $Fe_2Tb_xDy_{1-x}$ compound), enable efficient energy and information conversion between electromagnetic and mechanical energy[7-9]. Furthermore, Fe_2RE compounds have maximum strain characteristics among giant magnetostrictive materials[10,11]. Additionally, the intermetallic compounds made of RE elements, the transition metal Fe, and a third light element B (e.g., $Nd_2Fe_{14}B$, $Dy_2Fe_{14}B$, and $Tb_2Fe_{14}B$) have excellent magnetic properties as permanent magnets, widely used in various industries, including electronic information, electrical machine, and medical equipment[12-17]. The reliable phase diagrams and thermodynamic properties of the Fe-RE binary systems are essential to better understand the effect of RE metals on the phase formation of the Fe-RE intermetallic compounds.

Konar *et al.* executed a systematic calculation of the Fe-RE binary systems by using a modified quasichemical model to describe the liquid phase considering the reported experimental results[18,19]. Although the calculated thermodynamic properties and phase equilibria of the Fe-RE binary systems were in agreement with the experimental information, Konar *et al.* did not consider the heat capacity of Fe_2RE and $Fe_{17}RE_2$ phases (e.g., Fe_2Tb, Fe_2Dy, Fe_2Er, Fe_2Lu, $Fe_{17}Lu_2$, and $Fe_{17}Y_2$) at low temperature (below 298 K) in their calculations[19]. Moreover, to ensure model compatibility inside the thermodynamic database in the Fe-RE-based systems. The description of the liquid phase reported by Konar *et al.*[18,19] needs to be revised to match thermodynamic calculations of the B-RE binary systems in our previous work[20-24]. In our earlier work, we also assessed the Fe-RE (RE = La, Ce, Pr, Nd, Sm, Gd, Tb, Dy, Ho, and Tm) binary systems[25-29]. In addition, the Fe-RE (RE = Pm, Eu, and Yb) binary systems have not been assessed because of a lack of the experimental data, while the Fe-Y binary system was investigated through the experimental determination and thermodynamic calculations[19].

This study focuses on the Fe-RE (RE = Er, Lu, and Y) binary systems by the CALPHAD method in consideration of experimental results and previous calculations. To improve our previous calculations of the Fe-RE (Tb and Dy) binary systems[27], the Gibbs energies of intermetallic compounds Fe_2Tb and Fe_2Dy were modified to eliminate the artificial break point in their heat capacity curves that appear in the earlier work. By combining our present evaluations with previous optimizations[25-29], we provide a comprehensive discussion of phase equilibria and thermodynamic characteristics of the Fe-RE binary systems.

LITERATURE INFORMATION

Fe-La and Fe-Ce

Several studies have experimentally investigated the Fe-La binary phase diagram[30-33]. These studies identified three peritectic reactions and one eutectic reaction, but stable intermetallic compounds were not observed. In addition, the thermodynamic properties in liquid Fe-La alloys were measured[34,35].

The Fe-Ce binary system was experimentally investigated by different researchers[36-41]. $Fe_{17}Ce_2$ and Fe_2Ce compounds were found to form through peritectic reactions. In terms of thermochemical properties of liquid Fe-Ce alloys, the enthalpy of mixing and the partial enthalpy of mixing of Fe and Ce were measured experimentally by different researchers[35,42-43], while the enthalpy of formation of $Fe_{17}Ce_2$ and Fe_2Ce was measured[44-45].

Thermodynamic calculation of the Fe-La system was performed by several researchers[18,46], and that of the Fe-Ce system was performed[18,47]. In our previous work, the Fe-La and Fe-Ce binary systems were reassessed in consideration of new measured experimental results[29]. The calculated results of these two binary systems[29] are consistent well with the experimental information.

Fe-Pr and Fe-Nd

The Fe-Pr binary system has been experimentally studied[48-50]. According to the review[51,52], $Fe_{17}Pr_2$ is the only stable phase. There are two peritectic reactions, one peritectoid reaction, and one eutectic reaction. The thermodynamic properties in liquid Fe-Pr alloys were determined[53], while the enthalpy of formation of $Fe_{17}Pr_2$ was reported in Refs[44,54].

Several researchers investigated the Fe-Nd binary system[55-59]. These experimental results[55-59] show that $Fe_{17}Nd_2$ is the only stable phase. However, the researchers[60,61] found that $Fe_{17}Nd_5$ is also a stable intermetallic compound, and then the Fe-Nd phase diagram was revised accordingly. Okamoto[62,63] reviewed the Fe-Nd binary system. The thermodynamic properties of liquid Fe-Pr alloys were determined[53], while the enthalpy of formation of $Fe_{17}Nd_2$ was reported[44,54].

The Fe-Pr binary system was calculated[18,64-66], while the Fe-Nd system was calculated by several authors[18,60,67-68] considering these two stable intermetallic compounds, $Fe_{17}Nd_2$ and $Fe_{17}Nd_5$. In our previous work, the Fe-Pr and Fe-Nd binary systems were re-optimized[25] considering new determined experimental results. The calculated results of these two binary systems[25] are in accordance with the experimental information.

Fe-Sm and Fe-Gd

The Fe-Sm binary system has been determined by several authors[69]. Three intermetallic compounds, $Fe_{17}Sm_2$, Fe_3Sm, and Fe_2Sm, are formed (L + fcc-Fe ↔ $Fe_{17}Sm_2$, L + $Fe_{17}Sm_2$ ↔ Fe_3Sm, L + Fe_3Sm ↔ Fe_2Sm). Using the high-temperature calorimetric method, the enthalpy of mixing and the partial enthalpy of mixing at 1,829 K were determined[70], while the enthalpy of formation of $Fe_{17}Sm_2$ was measured[44].

The Fe-Gd binary system has been studied experimentally[71-78]. According to these measurements, four $Fe_{17}Gd_2$, $Fe_{23}Gd_6$, Fe_3Gd, and Fe_2Gd intermetallic compounds are formed by the peritectic transformation. The thermodynamic properties of liquid Fe-Gd alloys were measured[53,79]. The enthalpy of formation of Fe_2Gd was reported[44,80]. The enthalpy of formation of $Fe_{17}Gd_2$, Fe_3Gd, and Fe_2Gd was determined[81].

The Fe-Sm binary system was calculated[18,82-83], and the Fe-Gd binary system was evaluated[19,84-86]. The Fe-Sm and Fe-Gd systems were reassessed in our previous work[26], and the calculations are in accordance with the experimental information.

Fe-Ho and Fe-Tm

Roe *et al.* investigated the Fe-Ho binary system[87]. $Fe_{17}Ho_2$, $Fe_{23}Ho_6$, and Fe_2Ho are formed by congruent melting, and Fe_3Ho forms through the peritectic transformation. Four eutectic reactions are separately

L ↔ $Fe_{17}Ho_2$ + fcc-Fe, L ↔ $Fe_{17}Ho_2$ + $Fe_{23}Ho_6$, L ↔ Fe_2Ho + Fe_3Ho, and L ↔ hcp-Ho + Fe_2Ho. Besides, the enthalpy of formation of Fe_2Ho was investigated[44], while those of $Fe_{17}Ho_2$ and $Fe_{23}Ho_6$ were reported[54].

Kolesnichenko *et al.* determined the Fe-Tm binary system[88]. Considering the review of Massalski[89], four phases exist in this system. Fe_2Tm is formed congruently from liquid phase at 1573 K, while $Fe_{17}Tm_2$, $Fe_{23}Tm_6$, and Fe_3Tm form by three peritectic transformation. The enthalpy of formation of $Fe_{17}Tm_2$ and Fe_2Tm was studied[44,54].

The Fe-Tm and Fe-Ho binary systems were evaluated in Refs[19,90,91]. A reassessment of these two binary systems was performed in our previous study[28], and the assessments are consistent well with the experimental information.

Fe-Tb and Fe-Dy

The Fe-Tb binary system has been studied[92,93]. However, the determined melting temperatures[93] show the large experimental errors (± 50 K and about 3 at.%). Based on the experiment results[92], Okamoto[94] reported the Fe-Tb binary system. Four $Fe_{17}Tb_2$, $Fe_{23}Tb_6$, Fe_3Tb, and Fe_2Tb intermetallic compounds are produced via the peritectic transformation at 1,585 K, 1,549 K, 1,485 K, and 1,460 K, respectively, and $Fe_{17}Tb_2$ is produced at 1,589 K by the congruent melting. A eutectic reaction (L ↔ $Fe_{17}Tb_2$+bcc-Fe) takes place according to the DTA results[95] at 1,574 K.

The Fe-Dy binary system has been determined[96]. Four $Fe_{17}Dy_2$, $Fe_{23}Dy_6$, Fe_3Dy, and Fe_2Dy intermetallic compounds were found[96-98]. According to the literature[96,99], there are two congruent transformations (L ↔ $Fe_{17}Dy_2$ and L ↔ Fe_3Dy), two peritectic transformations (L + $Fe_{17}Dy_2$ ↔ $Fe_{23}Dy_6$ and L + Fe_3Dy ↔ Fe_2Dy), and three eutectic transformations (L ↔ $Fe_{17}Dy_2$ + fcc-Fe, L ↔ $Fe_{23}Dy_6$ + Fe_3Dy, and L ↔ Fe_2Dy + hcp-Dy).

Ivanov *et al.* measured the enthalpy of mixing and the partial enthalpy of mixing of Fe, Tb, and Dy at 1,833 K[53]. The activities of Dy in Fe-Dy alloys between 1,273 K and 1,573 K were reported[100]. The heat capacity, the enthalpy difference $(H_T^0 - H_0^0)$ and the entropy of formation (S_T^0) of Fe Tb and Fe Dy at low temperature (below 300 K) were measured[101]. Furthermore, the enthalpy of formation of $Fe_{17}Tb_2$ and $Fe_{17}Dy_2$ was measured[54]. The enthalpy of formation of Fe_2Tb, $Fe_{17}Tb_2$, Fe_2Dy, and $Fe_{17}Dy_2$ was recently measured to be -5.5 ± 2.4, -2.1 ± 3.1, -1.6 ± 2.9, and -5.3 ± 1.7 kJ/mol-atom[102], respectively. Similarly, the enthalpy of formation of Fe_2Dy, Fe_3Dy, and $Fe_{17}Dy_2$ was reported[103]. Using ab initio calculation, the enthalpy of formation of Fe_2Dy was reported to be -7.7 kJ/mol-atom[44].

The Fe-Tb and Fe-Dy binary systems were calculated by several authors[19,83,104,105]. In our previous work, a thermodynamic reassessment of the Fe-RE (RE = Tb and Dy) systems was conducted[27]. However, the heat capacity curves of Fe_2Tb and Fe_2Dy show artificial break points at 120 K due to the unreasonable expressions of their Gibbs energies. Therefore, the Gibbs energies of Fe_2Tb and Fe_2Dy were reassessed in this work based on the previous calculations[27].

Fe-Er

Buschow and Goot[106] investigated the Fe-Er binary phase diagram, and found $Fe_{17}Er_2$, $Fe_{23}Er_6$, Fe_3Er, and Fe_2Er. Meyer[107] studied the Fe-Er binary system, but the melting temperatures of these intermetallic compounds determined by Meyer[107] are much lower (about 70 K) than the results[106]. Subsequently, Kolesnikov *et al.*[108] re-determined the Fe-Er binary system and confirmed the reported results[106]. Furthermore, the experimental results[106-108] were reviewed by Okamoto[109]. The experimental results[106-108]

show two eutectic transformations (L ↔ $Fe_{17}Er_2$ + $Fe_{23}Er_6$ at 1,588 K and L ↔ Fe_2Er + hcp-Er at 1,188 K). $Fe_{17}Er_2$, $Fe_{23}Er_6$, and Fe_3Er are produced by three peritectic transformations (L + fcc-Fe ↔ $Fe_{17}Er_2$ at 1628 K, L + Fe_3Er ↔ $Fe_{23}Er_6$ at 1,603 K, and L + Fe_2Er ↔ Fe_3Er at 1,618 K), while Fe_2Er melts congruently at 1,633 K. The solubility in terminal solid solution phases (hcp-Er, fcc-Fe, and bcc-Fe) was not found in the literature.

The heat capacity of Fe_2Er at low temperature (8-300 K) was measured by Germano and Butera[101] using an adiabatic calorimeter, and thermodynamic functions [$(H_T^0 - H_0^0)$ and S_T^0] were obtained. The enthalpies of formation of the Fe-Er intermetallic compounds at different temperatures were measured[44,54,103]. Using indirect solution calorimetry, the enthalpies of formation of Fe_2Er and Fe_3Er were reported[103] at 1,100 K. The enthalpy of formation of $Fe_{17}Er_2$ was studied[54], while that of Fe_2Er was determined[44].

The Fe-Er binary system was calculated by several researchers[19,110-112]. It was pointed out that the magnetism of the Fe-Er intermetallic compounds was not considered in the calculation[110]. Considering the experimental heat capacity of Fe_2Er[101], the Fe-Er binary system was re-evaluated[111]. Although the calculations[111] are consistent with the results[106], the obtained heat capacity of Fe_2Er at low temperature (below 30 K) displays a noticeable deviation from the experimental results[101]. Besides, $Fe_{17}Er_2$ and Fe_3Er are decomposed at low temperatures (below 600 K)[112], which are contradictory to the experimental information. Therefore, the Fe-Er binary system is re-assessed in this study.

Fe-Lu

The Fe-Lu binary system has been studied[88], and four $Fe_{17}Lu_2$, $Fe_{23}Lu_6$, Fe_3Lu, and Fe_2Lu intermetallic compounds were found. There are three peritectic reactions (1,593 K, 1,563 K, and 1,583 K), which are corresponding to the formation of $Fe_{17}Lu_2$, $Fe_{23}Lu_6$, and Fe_3Lu, respectively. The congruent reaction at 1,618 K is corresponding to the formation of Fe_2Lu. Two eutectic transformations are L ↔ Fe_2Lu + hcp-Lu at 1,243 K and 75 at.% Lu, and L ↔ $Fe_{23}Lu_6$ + $Fe_{17}Lu_2$ at 1,548 K and 17.8 at.% Lu, respectively. The solubility in terminal solid solution was not measured in the literature.

The thermodynamic properties in liquid Fe-Lu alloys were determined at 1,950 K[53]. The heat capacity, the enthalpy difference $(H_T^0 - H_0^0)$, and the entropy of formation (S_T^0) of Fe_2Lu at low temperature (10-300 K) were measured[101]. Tereshina and Andreev[113] investigated the heat capacity of $Fe_{17}Lu_2$ at low temperature. The enthalpy of formation of Fe_2Lu was studied[54], while that of Fe_2Lu was reported[44].

The Fe-Lu binary system has been calculated[90]. However, the calculated thermodynamic properties including the partial enthalpy of mixing and the enthalpy of mixing are inconsistent with new measured data[53]. Thus, the Fe-Er binary system needs to be reassessed.

Fe-Y

The Fe-Y binary system has been investigated experimentally[114,115]. Due to the limitation of the purity of raw materials and experimental equipment, the experimental results[114] are not acceptable. Domagala *et al.* determined the eutectic reaction (L ↔ hcp-Y + Fe_2Y at 1,173 K) by metallography and X-ray diffraction[115]. The intermetallic compounds $Fe_{17}Y_2$, $Fe_{23}Y_6$, and Fe_3Y are produced by congruent reactions at 1,673 ± 25 K, 1,573 K, and 1,608 K, respectively. Gscheidner[116] and Kubaschewski[117] assessed the Fe-Y system in consideration of the experimental information[115]. The most recent evaluation of the Fe-Y system was carried out[118]. However, this evaluation focused only on the information of intermetallic compounds. Hellawell[119] reported that the solubility of 1 at.% Y reduces the transformation temperature [fcc(γ-Fe)/bcc(δ-Fe)], but Kubaschewski[117] still considered that the effect of Y on the transformation

[fcc(γ-Fe)/bcc(δ-Fe)] was not known. According to Buschow[120], $Fe_{17}Y_2$ has two modifications, the rhombohedral Th_2Zn_{17} and the hexagonal Th_2Ni_{17}. However, the temperature of this structure transformation was not reported, and thus $Fe_{17}Y_2$ was treated as a single phase in this work. It was found that the maximum solubility of Fe in hcp-Y is 1.5 at.% at 1173 K, but that of Y in fcc-Fe is not more than 0.6 at.% at 1,623 K[115].

The thermodynamic properties in liquid Fe-Y alloys at 1,873 K were measured[121,122]. The experimental results[121] show that the minimum enthalpy of mixing at 1,873 K is -8.44 kJ/mol at around 47 at.% Y. The measured partial enthalpy of mixing of Y in liquid Fe-Y alloys in the Fe-rich part[122] is much less negative than the measured results[121].

The Gibbs energy of formation of $Fe_{17}Y_2$ was measured[54], and then the enthalpy of formation of $Fe_{17}Y_2$ was deduced. The Gibbs energies of formation of $Fe_{17}Y_2$, $Fe_{23}Y_6$, Fe_3Y, and Fe_2Y were studied[123] between 893 K and 1,271 K.

Dariel *et al.* studied experimentally the specific heat and the Curie temperature of Fe_2Y by using differential scanning calorimetry[124]. However, Dariel *et al.* did not report the specific heat data but only gave the Curie temperature of Fe_2Y to be 535 K[124]. The heat capacity of $Fe_{17}Y_2$ was reported[125] at low temperature (below 300 K). The activities of Fe and Y were determined[126] at 1,473 K and 1,573 K.

Thermodynamic optimization of the Fe-Y binary system was performed[127], and the calculated results are in accordance with the reported data[115]. However, the calculated thermodynamic properties show significant deviations from the reported data[121], and $Fe_{23}Y_6$ is produced by the peritectic reaction rather than the congruent reaction, which was determined by Domagala *et al.*[115]. Later, several authors[128-130] re-optimized the Fe-Y binary system. Unfortunately, the relevant thermodynamic parameters were not published[128-130]. Combining the reported experimental data and the calculations, Kardelass *et al.* used two different models to optimize the Fe-Y binary system[131]. Combining with the reported results[114-119] and thermodynamic calculations[127-131], Saenko *et al.* optimized the new thermodynamic parameters of this binary system[132]. The calculations[132] are reasonably accordant with the experimental results. However, the calculations[131,132] show considerable homogeneity ranges of Y_6Fe_{23} and YFe_2, which are not confirmed by the reported experimental results. The calculations[133] show that the temperature of L ↔ hcp-Y + Fe_2Y is inconsistent with the reported data[115], and the partial enthalpy of mixing of Fe is inconsistent with the data[121]. Besides, the measured heat capacity of $Fe_{17}Y_2$[125] was not considered in the calculations[133] at low temperature (10-300 K). Therefore, the Fe-Y binary system needs to be reassessed.

THERMODYNAMIC CALCULATION

Thermodynamic model

The Gibbs energy of solution phase φ (including liquid, fcc, bcc, and hcp) in the Fe-Tb, Fe-Dy, Fe-Er, Fe-Lu, and Fe-Y binary systems is described as:

$$G_m^{\varphi} = {}^0G_{Fe}^{\varphi}x_{Fe} + {}^0G_{RE}^{\varphi}x_{RE} + RT\sum_{i=RE,Fe} x_i \ln x_i + x_{RE}x_{Fe}\sum_{n=0} {}^nL_{RE,Fe}^{\varphi}(x_{RE} - x_{Fe})^n + {}^{mag}G_m^{\varphi} \quad (1)$$

$${}^nL_{RE,Fe}^{\varphi} = A_n + B_nT \quad (2)$$

$${}^{mag}G_m^{\varphi} = RT\ln(\beta_0 + 1)g(\tau) \quad (3)$$

Where ${}^0G_{Fe}^{\varphi}$ and ${}^0G_{RE}^{\varphi}$ present the Gibbs energy of pure Fe and RE in the structure of the solution phase φ, and their values are obtained from the database[134]. x_{RE} and x_{FE} are mole fractions of Fe and RE. R is the universal gas constant, and T is the absolute temperature in Kelvin. The interaction parameters ${}^nL_{RE,Fe}^{\varphi}$ are presented by two constants A_n and B_n, which are optimized. ${}^{mag}G_m^{\varphi}$ present the magnetic contribution to the molar Gibbs energy of the of the solution phase φ. τ is expressed as $\tau = T/T_C^{\varphi}$, which T_C^{φ} is the Curie temperature. Based on the proposed equation[135], $g(\tau)$ is expressed as:

$$g(\tau) = \begin{cases} 1 - \frac{1}{M}\left[\frac{79\tau^{-1}}{140p} + \frac{474}{497}\left(\frac{1}{p} - 1\right)\left(\frac{\tau^3}{6} + \frac{\tau^9}{135} + \frac{\tau^{15}}{600}\right)\right] & (\tau > 1) \\ -\frac{1}{M}\left[\frac{\tau^{-5}}{10} + \frac{\tau^{-15}}{315} + \frac{\tau^{-25}}{1500}\right] & (\tau < 1) \end{cases} \quad (4)$$

$$M = \frac{518}{1125} + \frac{11692}{15975}\left(\frac{1}{p} - 1\right) \quad (5)$$

in which p is a constant dependent on the structure of the solution phase φ (0.4 for the bcc phase and 0.28 for other phases).

$Fe_{17}RE_2$, $Fe_{23}RE_6$, Fe_3RE, and Fe_2RE, are considered to be stoichiometric compounds in the Fe-RE (RE = Tb, Dy, Er, Lu, and Y) binary systems due to the lack of their composition range data. The heat capacities of Fe_2Tb, Fe_2Er, Fe_2Dy, $Fe_{17}Lu_2$, Fe_2Lu, and $Fe_{17}Y_2$ were experimentally determined by Germano and Butera[99], Tereshina *et al.*[113] and Mandal *et al.*[125]. In this work, according to available experimental data on heat capacities, the Gibbs energies of Fe_2Tb, Fe_2Dy, Fe_2Er, Fe_2Lu, $Fe_{17}Lu_2$, and $Fe_{17}Y_2$ were described by using a thermodynamic model, which can establish well the heat capacities of intermetallic compounds from 0 K. This model was employed in our previous assessments of Fe_2Ce and $Fe_{17}Ce_2$[29]. The molar Gibbs energies of these intermetallic compounds Fe_fRE_g are presented as:

$$G_m^{Fe_fRE_g} = A + BT + CT^2 + 3R\left\{\frac{D}{2} + T\ln\left[1 - \exp\left(-\frac{D}{T}\right)\right]\right\} + {}^{mag}G_m^{Fe_fRE_g} \quad (6)$$

Where f and g are the stoichiometric numbers, and the parameters, A, B, C, and D, are to be assessed.

The molar Gibbs energies of $Fe_{17}Tb_2$, $Fe_{23}Tb_6$, Fe_3Tb, $Fe_{17}Dy_2$, $Fe_{23}Dy_6$, Fe_3Dy, $Fe_{17}Er_2$, $Fe_{23}Er_6$, Fe_3Er, $Fe_{23}Lu_6$, Fe_3Lu, $Fe_{23}Y_6$, Fe_3Y, and Fe_2Y can be expressed based on the Neumann-Kopp rule as:

$$G_{\mathrm{m}}^{\mathrm{Fe_q RE_b}} = \frac{b}{b+q}\,{}^{0}G_{\mathrm{RE}}^{\varphi} + \frac{q}{b+q}\,{}^{0}G_{\mathrm{Fe}}^{bcc} + J + KT + {}^{mag}G_{m}^{\mathrm{Fe_q RE_b}} \tag{7}$$

in which b and q represent the stoichiometric numbers, J and K represent the optimized parameters. ${}^{mag}G_{\mathrm{m}}^{\mathrm{Fe_f RE_g}}$ and ${}^{mag}G_{\mathrm{m}}^{\mathrm{Fe_q RE_b}}$, as shown in Equation (6) and Equation (7), are the magnetic contribution to the molar Gibbs energy, and the formula is expressed by Equation (3). T_C and β_0 of the Fe-RE intermetallic compounds used in the present work can be found in Tables 1-5, respectively.

Thermodynamic calculation

The parameters of all stable phases in the Fe-RE (RE = Tb, Dy, Er, Lu, and Y) binary systems were optimized using the PARROT module of Thermo-Calc software[136] considering the experimental information (e.g., phase equilibria, enthalpy of mixing, enthalpy of formation, and heat capacity) reported in the literature. As for the Fe-RE binary systems, the experimental data are relatively limited because of the experimental difficulties. However, the systematic trends were observed for the thermodynamic characteristics of the RE-B[24], RE-Mn[137,138], and RE-Ni[139] binary systems with the increasing of RE atomic numbers. The Fe-RE binary systems also show a similar systematic trend, which was considered in the present calculations. For example, because the experimental enthalpy of mixing of liquid Fe-Er alloys was not reported in the literature, which was estimated by Konar *et al.*[19] using the formula $[\Delta H_{mix,\mathrm{Fe-Er}} = \Delta H_{mix,\mathrm{Fe-Dy}} + 0.5(\Delta H_{mix,\mathrm{Fe-Lu}} - \Delta H_{mix,\mathrm{Fe-Dy}})]$, where $\Delta H_{mix,\mathrm{Fe-Lu}}$ and $\Delta H_{mix,\mathrm{Fe-Dy}}$ were obtained from the measured experimental results[98].

The thermodynamic parameters were optimized finally, as shown in Tables 1-5, respectively. The enthalpy of formation (including the reported experimental results and the calculated results by the CALPHAD method and first-principles calculation) and the crystal structure data of the Fe-RE intermetallic compounds are shown in the Supplementary Materials.

CALCULATED RESULTS

Fe-Tb and Fe-Dy

Thermodynamic parameters of liquid phase and Fe_2Tb and Fe_2Dy were assessed in consideration of the experimental results[101] and the calculations[27]. In this work, the calculated Fe-Tb binary system is compared with the measured data[92,93,95] and the calculations[104], as shown in Figure 1. The temperatures of invariant reactions in the Fe-Tb binary system are calculated as listed in Table 6. The present calculations agree with the reported calculations[27,104], and the optimized parameters are shown in Table 1.

The presently calculated enthalpy of mixing and partial enthalpy of mixing in liquid Fe-Tb alloys at 1,833 K are accordant well with the calculations[27], as shown in Figure 2 and Figure 3. The enthalpies of formation of the Fe-Tb intermetallic compounds are calculated at 298 K in Figure 4, which is in good accordance with the calculations[19,27,104,140] and the experimental data[54,102]. The presently calculated enthalpy of formation of Fe_2Tb is -9.005 kJ/mol-atom. As presented in Figure 5, the calculated thermodynamic properties [e.g., heat capacity, the entropy of formation, and enthalpy difference $(H_T^0 - H_0^0)$ of Fe Tb] are in accordance with the data[101] and show no artificial break point at 120 K in the heat capacity curve.

Table 1. Thermodynamic parameters in the Fe-Tb binary system

Phase	Thermodynamic parameters*	Reference
Liquid	${}^{0}L^{\mathrm{Liq}}_{\mathrm{Fe,Tb}} = -20115.512 - 3.2T$	This work
	${}^{1}L^{\mathrm{Liq}}_{\mathrm{Fe,Tb}} = -3332.5193 - 11.1T$	
	${}^{2}L^{\mathrm{Liq}}_{\mathrm{Fe,Tb}} = 660.3 - 8.1T$	
bcc-(Fe/Tb)	${}^{0}L^{\mathrm{bcc}}_{\mathrm{Fe,Tb}} = 58000$	[27]
hcp-(Tb)	${}^{0}L^{\mathrm{hcp}}_{\mathrm{Fe,Tb}} = 150000$	[27]
fcc-(Fe)	${}^{0}G^{\mathrm{fcc}}_{\mathrm{Tb}} = {}^{0}G^{\mathrm{hcp}}_{\mathrm{Tb}} + 5000$	[27]
	${}^{0}L^{\mathrm{fcc}}_{\mathrm{Fe,Tb}} = 75000$	
$Fe_{17}Tb_2$	$G_{\mathrm{m}}^{\mathrm{Fe_{17}Tb_2}} = -10343 + 1.668T + 0.8947\,{}^{0}G^{\mathrm{bcc}}_{\mathrm{Fe}} + 0.1053\,{}^{0}G^{\mathrm{hcp}}_{\mathrm{Tb}}$	This work
	$T_{\mathrm{C}}^{\mathrm{Fe_{17}Tb_2}} = 408,\ \beta_0^{\mathrm{Fe_{17}Tb_2}} = 0.167$	[2]
$Fe_{23}Tb_6$	$G_{\mathrm{m}}^{\mathrm{Fe_{23}Tb_6}} = -12501 + 0.355T + 0.7931\,{}^{0}G^{\mathrm{bcc}}_{\mathrm{Fe}} + 0.2069\,{}^{0}G^{\mathrm{hcp}}_{\mathrm{Tb}}$	This work
	$T_{\mathrm{C}}^{\mathrm{Fe_{23}Tb_6}} = 574,\ \beta_0^{\mathrm{Fe_{23}Tb_6}} = 0.010$	[2]
Fe_3Tb	$G_{\mathrm{m}}^{\mathrm{Fe_3Tb}} = -12008 - 0.277T + 0.75\,{}^{0}G^{\mathrm{bcc}}_{\mathrm{Fe}} + 0.25\,{}^{0}G^{\mathrm{hcp}}_{\mathrm{Tb}}$	This work
	$T_{\mathrm{C}}^{\mathrm{Fe_3Tb}} = 652,\ \beta_0^{\mathrm{Fe_3Tb}} = 0.426$	[2]
Fe_2Tb	$G_{\mathrm{m}}^{\mathrm{Fe_2Tb}} = -14540 - 4.332T - 0.0074T^2 + 3\mathrm{R}\left\{\frac{185}{2} + T\ln\left[1 - \exp\left(-\frac{185}{T}\right)\right]\right\}$	This work
	$T_{\mathrm{C}}^{\mathrm{Fe_2Tb}} = 704,\ \beta_0^{\mathrm{Fe_2Tb}} = 0.762$	[2]

*The Gibbs energies (J/mol) of Fe and Tb with liquid, bcc, fcc, and hcp structures are given by Dinsdale [134]. The unit of temperature (T) is Kelvin (K).

Table 2. Thermodynamic parameters in the Fe-Dy binary system

Phase	Thermodynamic parameters*	Reference
Liquid	${}^{0}L^{\mathrm{Liq}}_{\mathrm{Dy,Fe}} = -32524.791 + 10.7T$	This work
	${}^{1}L^{\mathrm{Liq}}_{\mathrm{Dy,Fe}} = 14150.219 - 1.17T$	
	${}^{2}L^{\mathrm{Liq}}_{\mathrm{Dy,Fe}} = 422.595 - 8.2T$	
bcc-(Fe/Dy)	${}^{0}L^{\mathrm{fcc}}_{\mathrm{Dy,Fe}} = 38000$	[27]
hcp-(Dy)	${}^{0}L^{\mathrm{hcp}}_{\mathrm{Dy,Fe}} = 100000$	[27]
fcc-(Fe)	${}^{0}G^{\mathrm{fcc}}_{\mathrm{Dy}} = {}^{0}G^{\mathrm{hcp}}_{\mathrm{Dy}} + 5000$	[27]
	${}^{0}L^{\mathrm{fcc}}_{\mathrm{Dy,Fe}} = 38000$	
$Fe_{17}Dy_2$	$G_{\mathrm{m}}^{\mathrm{Fe_{17}Dy_2}} = -12882 + 3.744T + 0.8947\,{}^{0}G^{\mathrm{bcc}}_{\mathrm{Fe}} + 0.1053\,{}^{0}G^{\mathrm{hcp}}_{\mathrm{Dy}}$	This work
	$T_{\mathrm{C}}^{\mathrm{Fe_{17}Dy_2}} = 371,\ \beta_0^{\mathrm{Fe_{17}Dy_2}} = 0.161$	[2]
$Fe_{23}Dy_6$	$G_{\mathrm{m}}^{\mathrm{Fe_{23}Dy_6}} = -15700 + 3.909T + 0.7931\,{}^{0}G^{\mathrm{bcc}}_{\mathrm{Fe}} + 0.2069\,{}^{0}G^{\mathrm{hcp}}_{\mathrm{Dy}}$	This work
	$T_{\mathrm{C}}^{\mathrm{Fe_{23}Dy_6}} = 534,\ \beta_0^{\mathrm{Fe_{23}Dy_6}} = 0.100$	[2]
Fe_3Dy	$G_{\mathrm{m}}^{\mathrm{Fe_3Dy}} = -15506 + 3.101T + 0.75\,{}^{0}G^{\mathrm{bcc}}_{\mathrm{Fe}} + 0.25\,{}^{0}G^{\mathrm{hcp}}_{\mathrm{Dy}}$	This work
	$T_{\mathrm{C}}^{\mathrm{Fe_3Lu}} = 606,\ \beta_0^{\mathrm{Fe_3Lu}} = 0.493$	[2]
Fe_2Dy	$G_{\mathrm{m}}^{\mathrm{Fe_2Dy}} = -17860 - 5.419T - 0.00672T^2 + 3\mathrm{R}\left\{\frac{210}{2} + T\ln\left[1 - \exp\left(-\frac{210}{T}\right)\right]\right\}$	This work
	$T_{\mathrm{C}}^{\mathrm{Fe_2Dy}} = 635,\ \beta_0^{\mathrm{Fe_2Dy}} = 0.890$	[2]

*The Gibbs energies (J/mol) of Fe and Dy with liquid, bcc, fcc, and hcp structures are given by Dinsdale [134]. The unit of temperature (T) is Kelvin (K).

Table 3. Thermodynamic parameters in the Fe-Er binary system

Phase	Thermodynamic parameters*	Reference
Liquid	${}^{0}L^{\mathrm{Liq}}_{\mathrm{Er,Fe}} = -37100 + 12.1T$	This work
	${}^{1}L^{\mathrm{Liq}}_{\mathrm{Er,Fe}} = 15300 - 15.2T$	
	${}^{2}L^{\mathrm{Liq}}_{\mathrm{Er,Fe}} = -3500 + 2.8T$	
bcc-(Fe)	${}^{0}L^{\mathrm{bcc}}_{\mathrm{Er,Fe}} = 75000$	This work
hcp-(Er)	${}^{0}L^{\mathrm{hcp}}_{\mathrm{Er,Fe}} = 80000$	This work
fcc-(Fe)	${}^{0}G^{\mathrm{fcc}}_{\mathrm{Fe}}$ cited from SGTE database	[134]
$Fe_{17}Er_2$	$G^{\mathrm{Fe_{17}Er_2}}_{\mathrm{m}} = -11321 + 4.4546T + 0.8947\,{}^{0}G^{\mathrm{bcc}}_{\mathrm{Fe}} + 0.1053\,{}^{0}G^{\mathrm{hcp}}_{\mathrm{Er}}$	This work
	$T^{\mathrm{Fe_{17}Er_2}}_{\mathrm{C}} = 305,\ \beta^{\mathrm{Fe_{17}Er_2}}_{0} = 0.165$	[2]
$Fe_{23}Er_6$	$G^{\mathrm{Fe_{23}Er_6}}_{\mathrm{m}} = -14250 + 4.4056T + 0.7931\,{}^{0}G^{\mathrm{bcc}}_{\mathrm{Fe}} + 0.2069\,{}^{0}G^{\mathrm{hcp}}_{\mathrm{Er}}$	This work
	$T^{\mathrm{Fe_{23}Er_6}}_{\mathrm{C}} = 494,\ \beta^{\mathrm{Fe_{23}Er_6}}_{0} = 0.071$	[2]
Fe_3Er	$G^{\mathrm{Fe_3Er}}_{\mathrm{m}} = -14347 + 3.6854T + 0.75\,{}^{0}G^{\mathrm{bcc}}_{\mathrm{Fe}} + 0.25\,{}^{0}G^{\mathrm{hcp}}_{\mathrm{Er}}$	This work
	$T^{\mathrm{Fe_3Er}}_{\mathrm{C}} = 552,\ \beta^{\mathrm{Fe_3Er}}_{0} = 0.452$	[2]
Fe_2Er	$G^{\mathrm{Fe_2Er}}_{\mathrm{m}} = -17458 - 6.4717T + 0.00538T^2 + 3\mathrm{R}\left\{\frac{210}{2} + T\ln\left[1 - \exp\left(-\frac{210}{T}\right)\right]\right\}$	This work
	$T^{\mathrm{Fe_2Er}}_{\mathrm{C}} = 587,\ \beta^{\mathrm{Fe_2Er}}_{0} = 0.802$	[2]

*The Gibbs energies (J/mol) of Fe and Er with liquid, bcc, fcc, and hcp structures are given by Dinsdale [134]. The unit of temperature (T) is Kelvin (K).

Table 4. Thermodynamic parameters in the Fe-Lu binary system

Phase	Thermodynamic parameters*	Reference
Liquid	${}^{0}L^{\mathrm{Liq}}_{\mathrm{Fe,Lu}} = -44158.73 + 14.99T$	This work
	${}^{1}L^{\mathrm{Liq}}_{\mathrm{Fe,Lu}} = -19539.28 + 9.78T$	
	${}^{2}L^{\mathrm{Liq}}_{\mathrm{Fe,Lu}} = -1356.5296 + 3.17T$	
bcc-(Fe)	${}^{0}G^{\mathrm{bcc}}_{\mathrm{Fe}}$ cited from SGTE database	[134]
hcp-(Lu)	${}^{0}L^{\mathrm{hcp}}_{\mathrm{Fe,Lu}} = 50000$	This work
fcc-(Fe)	${}^{0}G^{\mathrm{fcc}}_{\mathrm{Fe}}$ cited from SGTE database	[134]
$Fe_{17}Lu_2$	$G^{\mathrm{Fe_{17}Lu_2}}_{\mathrm{m}} = -11769 - 2.856T - 0.002T^2 + 3\mathrm{R}\left\{\frac{240}{2} + T\ln\left[1 - \exp\left(-\frac{240}{T}\right)\right]\right\}$	This work
	$T^{\mathrm{Fe_{17}Lu_2}}_{\mathrm{C}} = 268,\ \beta^{\mathrm{Fe_{17}Lu_2}}_{0} = 0.206$	[2]
$Fe_{23}Lu_6$	$G^{\mathrm{Fe_{23}Lu_6}}_{\mathrm{m}} = -15608 + 4.769T + 0.7931\,{}^{0}G^{\mathrm{bcc}}_{\mathrm{Fe}} + 0.2069\,{}^{0}G^{\mathrm{hcp}}_{\mathrm{Lu}}$	This work
	$T^{\mathrm{Fe_{23}Lu_6}}_{\mathrm{C}} = 481,\ \beta^{\mathrm{Fe_{23}Lu_6}}_{0} = 0.140$	[2]
Fe_3Lu	$G^{\mathrm{Fe_3Lu}}_{\mathrm{m}} = -15802 + 4.039T + 0.75\,{}^{0}G^{\mathrm{bcc}}_{\mathrm{Fe}} + 0.25\,{}^{0}G^{\mathrm{hcp}}_{\mathrm{Lu}}$	This work
	$T^{\mathrm{Fe_3Lu}}_{\mathrm{C}} = 606,\ \beta^{\mathrm{Fe_3Lu}}_{0} = 0.493$	[2]
Fe_2Lu	$G^{\mathrm{Fe_2Lu}}_{\mathrm{m}} = -18167 - 4.61T + 0.00313T^2 + 3\mathrm{R}\left\{\frac{230}{2} + T\ln\left[1 - \exp\left(-\frac{230}{T}\right)\right]\right\}$	This work
	$T^{\mathrm{Fe_2Lu}}_{\mathrm{C}} = 596,\ \beta^{\mathrm{Fe_2Lu}}_{0} = 0.578$	[2]

*The Gibbs energies (J/mol) of Fe and Lu with liquid, bcc, fcc, and hcp structures are given by Dinsdale [134]. The unit of temperature (T) is Kelvin (K).

Table 5. Thermodynamic parameters in the Fe-Y binary system

Phase	Thermodynamic parameters*	Reference
Liquid	${}^{0}L^{\mathrm{Liq}}_{\mathrm{Fe,Y}} = -33500 + 17.5T$	This work
	${}^{1}L^{\mathrm{Liq}}_{\mathrm{Fe,Y}} = -2800 + 1.2T$	
	${}^{2}L^{\mathrm{Liq}}_{\mathrm{Fe,Y}} = 9000 - 4.0T$	
bcc-(Fe/Y)	${}^{0}L^{\mathrm{bcc}}_{\mathrm{Fe,Y}} = 63000$	This work
hcp-(Y)	${}^{0}L^{\mathrm{hcp}}_{\mathrm{Fe,Y}} = 34000$	This work
fcc-(Fe)	${}^{0}G^{\mathrm{fcc}}_{\mathrm{Y}} = {}^{0}G^{\mathrm{hcp}}_{\mathrm{Y}} + 5000$	[142]
	${}^{0}L^{\mathrm{fcc}}_{\mathrm{Fe,Y}} = 60000$	This work
$Fe_{17}Y_2$	$G^{\mathrm{Fe_{17}Y_2}}_{\mathrm{m}} = -11250 - 1.538T + 0.0061T^2 + 3\mathrm{R}\left\{\frac{270}{2} + T\ln\left[1 - \exp\left(-\frac{270}{T}\right)\right]\right\}$	This work
	$T^{\mathrm{Fe_{17}Y_2}}_{\mathrm{C}} = 324,\ \beta^{\mathrm{Fe_{17}Y_2}}_{0} = 0.204$	[132]
$Fe_{23}Y_6$	$G^{\mathrm{Fe_{23}Y_6}}_{\mathrm{m}} = -11910 + 3.583T + 0.7931{}^{0}G^{\mathrm{bcc}}_{\mathrm{Fe}} + 0.2069{}^{0}G^{\mathrm{hcp}}_{\mathrm{Y}}$	This work
	$T^{\mathrm{Fe_{23}Y_6}}_{\mathrm{C}} = 481,\ \beta^{\mathrm{Fe_{23}Y_6}}_{0} = 0.139$	[132]
Fe_3Y	$G^{\mathrm{Fe_3Y}}_{\mathrm{m}} = -11500 + 2.784T + 0.75{}^{0}G^{\mathrm{bcc}}_{\mathrm{Fe}} + 0.25{}^{0}G^{\mathrm{hcp}}_{\mathrm{Y}}$	This work
	$T^{\mathrm{Fe_3Y}}_{\mathrm{C}} = 569,\ \beta^{\mathrm{Fe_3Y}}_{0} = 0.581$	[132]
Fe_2Y	$G^{\mathrm{Fe_2Y}}_{\mathrm{m}} = -11885 + 3.068T + 0.6667{}^{0}G^{\mathrm{bcc}}_{\mathrm{Fe}} + 0.3333{}^{0}G^{\mathrm{hcp}}_{\mathrm{Y}}$	This work
	$T^{\mathrm{Fe_2Y}}_{\mathrm{C}} = 542,\ \beta^{\mathrm{Fe_2Y}}_{0} = 0.574$	[132]

*The Gibbs energies (J/mol) of Fe and Y with liquid, bcc, fcc, and hcp structures are given by Dinsdale [134]. The unit of temperature (*T*) is Kelvin (K).

Figure 6 compares the presently calculated Fe-Dy binary system with the data[96] and the calculations[104,105]. The calculated temperatures of the invariant reactions in Fe-Dy binary system were seen in Table 7. The presently calculated results agree well with the reported results[96] and the calculations[104,105].

The presently calculated partial enthalpy of mixing and enthalpy of mixing in liquid Fe-Dy alloys are consistent with the calculations[27], as given in Figure 7 and Figure 8, respectively. In Figure 9, the enthalpies of formation of the Fe-Dy intermetallic compounds in the present calculation at 298 K agree well with the calculations[19,27,44,83,104,105,141] and the experimental data[54,102,103]. The enthalpy of formation of Fe_2Dy is calculated as -12.327 kJ/mol-atom. Additionally, the calculated thermodynamic properties [e.g., heat capacity, entropy of formation and enthalpy difference compares] of Fe_2Dy, as shown in Figure 10, are much better accordance with the results[101] and show no artificial break point in the heat capacity curve.

Fe-Er

Figure 11 displays the presently calculated Fe-Er binary system with the earlier calculations[110-112] and the experimental results[106-108]. As can be seen, $Fe_{17}Er_2$, $Fe_{23}Er_6$, Fe_3Er, and Fe_2Er are stable at room temperature, but some compounds are unstable at low temperature in the literature[112]. The presently calculated liquidus and solidus in Figure 11(B) agree with the experimental data[106-108]. Table 8 compares the calculated results of invariant reactions together with the experimental results. The temperatures and compositions of two eutectic reactions, L ↔ $Fe_{17}Er_2$ + $Fe_{23}Er_6$ and L ↔ Fe_2Er + hcp-Er, are calculated to be 1,601.8 K and 18.2 at.% Er and 1,185.6 K and 66.9 at.% Er, respectively. A congruent reaction of Fe_2Er (L ↔ Fe_2Er) happens at 1640.4 K, and those of four peritectic reactions (L + bcc-Fe ↔ fcc-Fe, L + fcc-Fe ↔ $Fe_{17}Er_2$, L + Fe_3Er ↔ $Fe_{23}Er_6$, and L + Fe_2Er ↔ Fe_3Er) are calculated to be 1,663.2 K, 1,625.1 K, 1,601.8 K, and 1,615.0 K, respectively, agreeing well with the results[106-108].

Table 6. Invariant reactions of the Fe-Tb binary system

Reactions	Reaction type	Temperature (K)	Composition (x_{Tb}^{L})	Reference
bcc(δ-Fe) ↔ fcc(γ-Fe) + L	Metatectic	1667.0	0.120	[94] (exp.)
		1665.1	0.080	[104] (cal.)
		1664.0	0.100	[27] (cal.)
		1666.9	0.050	This work (cal.)
$Fe_{17}Tb_2$ + fcc(γ-Fe) ↔ bcc(α-Fe)	Peritectoid	1185.0		[94] (exp.)
		1184.8		[104] (cal.)
		1185.0		[27] (cal.)
		1184.8		This work (cal.)
L ↔ $Fe_{17}Tb_2$ + fcc(γ-Fe)	Eutectic	1574.0	0.075	[95] (exp.)
		1579.0	0.082	[19] (cal.)
		1576.0	0.075	[27] (cal.)
		1575.0	0.076	This work (cal.)
L ↔ $Fe_{17}Tb_2$	Congruent	1589.0	0.105	[95] (exp.)
		1585.0	0.105	[19] (cal.)
		1586.0	0.105	[27] (cal.)
		1587.5	0.105	This work (cal.)
L ↔ $Fe_{17}Tb_2$ + $Fe_{23}Tb_6$	Eutectic	1549.0	0.216	[92] (exp.)
		1547.0		[95] (exp.)
		1542.7	0.212	[104] (cal.)
		1546.0	0.190	[19] (cal.)
		1546.0	0.208	[27] (cal.)
		1546.5	0.167	This work (cal.)
L ↔ $Fe_{23}Tb_6$	Congruent	1547.0	0.207	[19] (cal.)
		1561.1	0.207	This work (cal.)
L+ $Fe_{23}Tb_6$ ↔ Fe_3Tb	Peritectic	1485.0	0.349	[92] (exp.)
		1473.1	0.361	[104] (cal.)
		1481.0	0.388	[19] (cal.)
		1485.0	0.340	[27] (cal.)
		1486.0	0.319	This work (cal.)
L + Fe_3Tb ↔ Fe_2Tb	Peritectic	1460.0	0.412	[92] (exp.)
		1456.6	0.403	[104] (cal.)
		1459.0	0.424	[19] (cal.)
		1460.0	0.405	[27] (cal.)
		1462.7	0.348	This work (cal.)
L ↔ Fe_2Tb + hcp-Tb	Eutectic	1120.0	0.720	[92] (exp.)
		1123.0	0.687	[104] (cal.)
		1122.0	0.700	[19] (cal.)
		1120.0	0.690	[27] (cal.)
		1117.1	0.675	This work (cal.)

The available experimental enthalpy of mixing was not reported. The enthalpy of mixing is calculated at 1833 K and compared with the calculations[19,110-112] in Figure 12. Figure 13 is the presently calculated enthalpy of formation of the Fe-Er intermetallic compounds together with the results[44,54,103] and the calculations[19,110-112,140,141]. The presently calculated enthalpy of formation of $Fe_{17}Er_2$, $Fe_{23}Er_6$, Fe_3Er, and Fe_2Er are -3.255, -7.216, -8.881, and -11.611 kJ/mol-atom, respectively, which are accordant with the experimental results[54,103]. The presently calculated enthalpy of formation of Fe_2Er is more negative than the measured results[44]. On the other hand, it should be pointed out that the measured data[44] are significantly less negative than that measured data[103]. The heat capacity, entropy of formation, and enthalpy difference of Fe_2Er are calculated to be compared with the experimental results[101] and the calculations[110-112] in Figure 14A-C, respectively. The presently calculated heat capacity of Fe_2Er is much better consistent with the experimental data[101] than the earlier calculations[110-112].

Fe-Lu

Figure 15 presents the calculated Fe-Lu binary system, the calculations[90], and the experimental results[88]. It is observed in Figure 15A that $Fe_{17}Lu_2$ decomposes at low temperature according to the calculations[90], while $Fe_{17}Lu_2$, $Fe_{23}Lu_6$, Fe_3Lu, and Fe_2Lu are stable down to room temperature in this work. As displayed in

Table 7. Invariant reactions of the Fe-Dy binary system

Reactions	Reaction type	Temperature (K)	Composition (x^L_{Dy})	Reference
bcc(δ-Fe) ↔ fcc(γ-Fe) + L	Metatectic	1663.0	0.085	[99] (exp.)
		1667.9	0.070	[104] (cal.)
		1667.5	0.060	[105] (cal.)
		1662.0	0.060	[27] (cal.)
		1664.0	0.055	This work (cal.)
$Fe_{17}Dy_2$ + fcc(γ-Fe) ↔ bcc(α-Fe)	Peritectoid	1183.0		[99] (exp.)
		1184.8		[104] (cal.)
		1184.8		[105] (cal.)
		1185.0		[27] (cal.)
		1184.8		This work (cal.)
L ↔ $Fe_{17}Dy_2$ + fcc(γ-Fe)	Eutectic	1633.0	0.090	[96] (exp.)
		1641.7	0.083	[104] (cal.)
		1630.7	0.078	[105] (cal.)
		1639.0		[83] (cal.)
		1638.0	0.074	[19] (cal.)
		1634.0	0.080	[27] (cal.)
		1630.0	0.066	This work(cal.)
L ↔ $Fe_{17}Dy_2$	Congruent	1648.0	0.105	[96] (exp.)
		1644.8	0.105	[104] (cal.)
		1637.5	0.105	[105] (cal.)
		1640.0	0.105	[83] (cal.)
		1649.0	0.105	[19] (cal.)
		1647.0	0.105	[27] (cal.)
		1651.0	0.105	This work(cal.)
L + $Fe_{17}Dy_2$ ↔ $Fe_{23}Dy_6$	Peritectic	1563.0	0.212	[96] (exp.)
		1561.9	0.218	[105] (cal.)
		1574.0	0.210	[19] (cal.)
		1565.0	0.212	[27] (cal.)
		1567.4	0.209	This work (cal.)
L ↔ $Fe_{23}Dy_6$ + Fe_3Dy	Eutectic	1558.0	0.225	[96] (exp.)
		1561.0	0.225	[105] (cal.)
		1573.0	0.215	[19] (cal.)
		1557.0	0.221	[27] (cal.)
		1567.3	0.212	This work (cal.)
L ↔ Fe_3Dy	Congruent	1578.0	0.250	[96] (exp.)
		1581.8	0.250	[104] (cal.)
		1563.5	0.250	[105] (cal.)
		1580.0	0.250	[83] (cal.)
		1580.0	0.250	[19] (cal.)
		1579.0	0.250	[27] (cal.)
		1576.4	0.250	This work (cal.)
L + Fe_3Dy ↔ Fe_2Dy	Peritectic	1543.0	0.401	[96] (exp.)
		1542.9	0.363	[104] (cal.)
		1535.9	0.335	[105] (cal.)
		1545.0		[83] (cal.)
		1548.0	0.339	[19] (cal.)
		1547.0	0.390	[27] (cal.)
		1545.5	0.335	This work (cal.)
L ↔ Fe_2Dy + hcp-Dy	Eutectic	1163.0	0.715	[96] (exp.)
		1162.1	0.716	[104] (cal.)
		1165.3	0.717	[105] (cal.)
		1164.0	0.730	[83] (cal.)
		1161.0	0.691	[19] (cal.)
		1161.0	0.710	[27] (cal.)
		1160.0	0.696	This work(cal.)

Figure 15B, the present calculations agree with the results[88]. Table 9 displays the calculated results of invariant reactions with the measured data[88]. The results of two eutectic reactions, L ↔ $Fe_{17}Lu_2$ + $Fe_{23}Lu_6$ and L ↔ Fe_2Lu + hcp-Lu, are calculated to be 1,559.9 K and 18.4 at.% Lu and 1,240.3 K and 64.2 at.% Lu, respectively. The congruent melting of Fe_2Lu (L ↔ Fe_2Lu) is calculated to be 1,619.6 K, while those of four peritectic reactions, L + bcc-Fe ↔ fcc-Fe, L + fcc-Fe ↔ $Fe_{17}Lu_2$, L + Fe_3Lu ↔ $Fe_{23}Lu_6$, and L + Fe_2Lu ↔ Fe_3Lu, are calculated to be 1,667.5 K, 1,590.1 K, 1,560.9 K, and 1,580.4 K, respectively. These present calculations

Table 8. Invariant reactions of the Fe-Er binary system

Reactions	Reaction type	Temperature (K)	Composition (x_{Er}^{L})	Reference
bcc(δ-Fe) ↔ fcc(γ-Fe) + L	Metatectic	1658.0	0.100	[106] (exp.)
		1667.5	0.081	[110] (cal.)
		1658.0	0.082	[111] (cal.)
		1658.0	0.089	[112] (cal.)
		1661.5	0.084	This work (cal.)
$Fe_{17}Er_2$ + fcc(γ-Fe) ↔ bcc(α-Fe)	Peritectoid	1184.8		This work
L + fcc(γ-Fe) ↔ $Fe_{17}Er_2$	Peritectic	1628.0	0.104	[106] (exp.)
		1616.0	0.105	[110] (cal.)
		1619.0	0.105	[111] (cal.)
		1626.0	0.108	[112] (cal.)
		1630.0	0.106	[19] (cal.)
		1625.1	0.106	This work (cal.)
L ↔ $Fe_{17}Er_2$ + $Fe_{23}Er_6$	Eutectic	1588.0	0.165	[106] (exp.)
		1599.0	0.174	[110] (cal.)
		1600.0	0.181	[111] (cal.)
		1600.5	0.178	[112] (cal.)
		1581.0	0.171	[19] (cal.)
		1601.8	0.182	This work (cal.)
L+ Fe_3Er ↔ $Fe_{23}Er_6$	Peritectic	1603.0	0.197	[106] (exp.)
		1601.0	0.191	[110] (cal.)
		1600.0	0.182	[111] (cal.)
		1602.7	0.190	[112] (cal.)
		1595.0	0.202	[19] (cal.)
		1602.7	0.189	This work (cal.)
L + Fe_2Er ↔ Fe_3Er	Peritectic	1618.0	0.248	[106] (exp.)
		1611.0	0.240	[110] (cal.)
		1611.0	0.235	[111] (cal.)
		1615.7	0.250	[112] (cal.)
		1612.0	0.279	[19] (cal.)
		1615.0	0.250	This work (cal.)
L ↔ Fe_2Er	Congruent	1633.0	0.333	[106] (exp.)
		1632.0	0.333	[110] (cal.)
		1633.0	0.333	[111] (cal.)
		1636.0	0.333	[112] (cal.)
		1633.0	0.333	[19] (cal.)
		1640.4	0.333	This work (cal.)
L ↔ Fe_2Er + hcp-Er	Eutectic	1188.0	0.700	[106] (exp.)
		1185.0	0.692	[110] (cal.)
		1189.0	0.719	[111] (cal.)
		1187.9	0.687	[112] (cal.)
		1189.0	0.684	[19] (cal.)
		1185.6	0.669	This work (cal.)

results are in accordance with the reported results[88].

Figure 16 shows the calculated enthalpy of mixing of liquid Fe-Lu alloys at 1,950 K with the measured results[53] and the calculations[90]. A significant deviation between the calculations[90] and the experimental data[53] is found, while the present calculations agree with the experimental data[53]. In Figure 17, the partial enthalpy of mixing of Fe and Lu in liquid Fe-Lu alloys is calculated and compared with the measured results[53] and the calculations[90]. It is obvious that our calculations are accordant well with the measured data[53], while the calculations[90] show large deviations.

Figure 18 depicts the calculated enthalpy of formation of the Fe-Lu compounds at 298 K with the measured results[44,54] and the calculations[19,90,140,141]. The enthalpy of formation of $Fe_{17}Lu_2$, $Fe_{23}Lu_6$, Fe_3Lu, and Fe_2Lu are calculated to be -3.69, -8.762, -10.615, and -11.957 kJ/mol-atom, respectively. The presently calculated enthalpy of formation of $Fe_{17}Lu_2$ is in accordance with the measured data[54], while the calculated that of Fe_2Lu is slightly lower than the measured data[44]. It is worth mentioning that the measured enthalpy of

Table 9. Invariant reactions of the Fe-Lu binary system

Reactions	Reaction type	Temperature (K)	Composition (x_{Lu}^{L})	Reference
L + bcc(δ-Fe) ↔ fcc(γ-Fe)	Peritectic	1667.0		[88] (exp.)
		1667.0		[90] (cal.)
		1667.5	0.070	This work (cal.)
$Fe_{17}Lu_2$ + fcc(γ-Fe) ↔ bcc(α-Fe)	Peritectoid	1185.0		[88] (exp.)
		1185.0		[90] (cal.)
		1184.8		This work (cal.)
L + fcc(γ-Fe) ↔ $Fe_{17}Lu_2$	Peritectic	1593.0	0.130	[88] (exp.)
		1593.0	0.090	[90] (cal.)
		1602.0	0.111	[19] (cal.)
		1590.1	0.105	This work(cal.)
L ↔ $Fe_{17}Lu_2$ + $Fe_{23}Lu_6$	Eutectic	1548.0	0.180	[88] (exp.)
		1549.0	0.158	[90] (cal.)
		1546.0	0.172	[19] (cal.)
		1559.9	0.184	This work (cal.)
L + Fe_3Lu ↔ $Fe_{23}Lu_6$	Peritectic	1563.0	0.196	[88] (exp.)
		1560.0	0.183	[90] (cal.)
		1560.0	0.202	[19] (cal.)
		1560.9	0.188	This work (cal.)
L + Fe_2Lu ↔ Fe_3Lu	Peritectic	1583.0	0.225	[88] (exp.)
		1581.0	0.229	[90] (cal.)
		1580.0	0.333	[19] (cal.)
		1580.4	0.241	This work (cal.)
L ↔ Fe_2Lu	Congruent	1618.0	0.333	[88] (exp.)
		1618.0	0.333	[90] (cal.)
		1620.0	0.333	[19] (cal.)
		1619.6	0.333	This work (cal.)
L ↔ Fe_2Lu + hcp-Lu	Eutectic	1243.0	0.750	[88] (exp.)
		1237.0	0.741	[90] (cal.)
		1249.0	0.670	[19] (cal.)
		1240.3	0.642	This work(cal.)

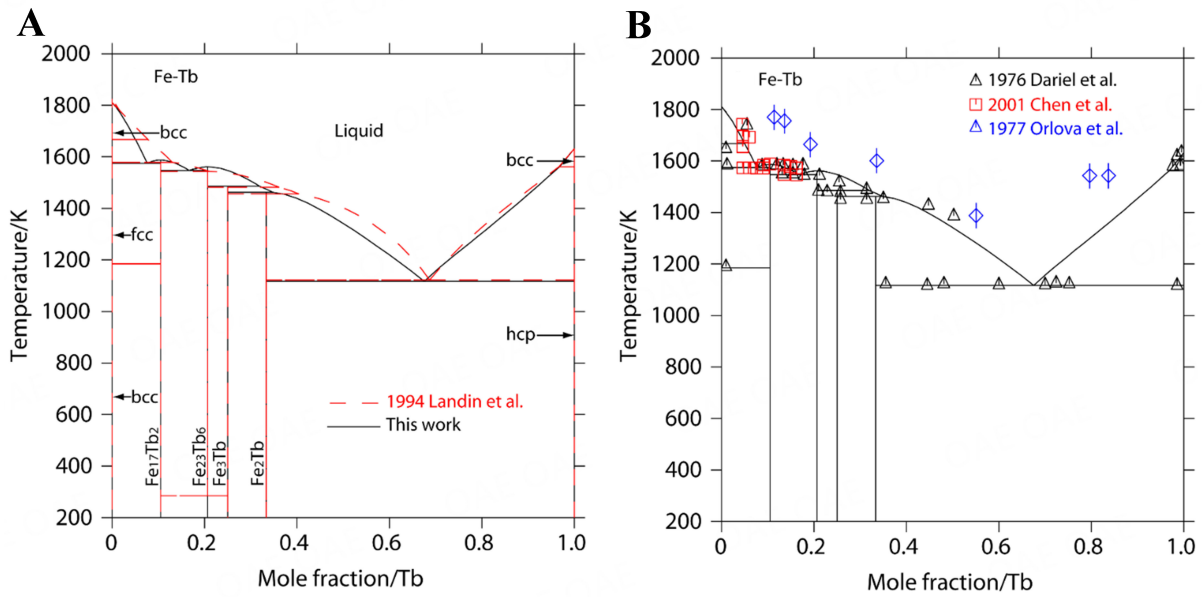

Figure 1. Calculated Fe-Tb binary phase diagram with (A) the calculations[104] and (B) the experimental data[92,93,95].

formation of Fe_2RE in the Fe-RE binary systems by the authors[44] is all less negative. Further experiments are still needed to determine the enthalpy of formation of the Fe-Lu intermetallic compounds.

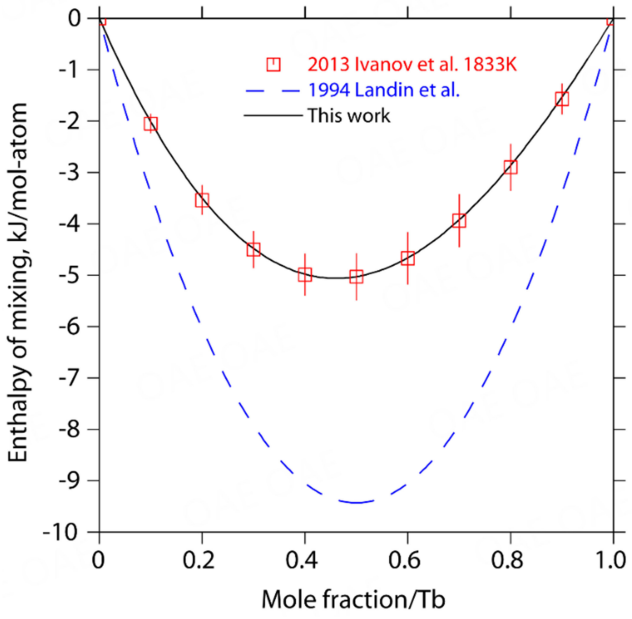

Figure 2. The calculated enthalpy of mixing of liquid Fe-Tb alloys at 1,833 K with the calculations[104] and the experimental data[53].

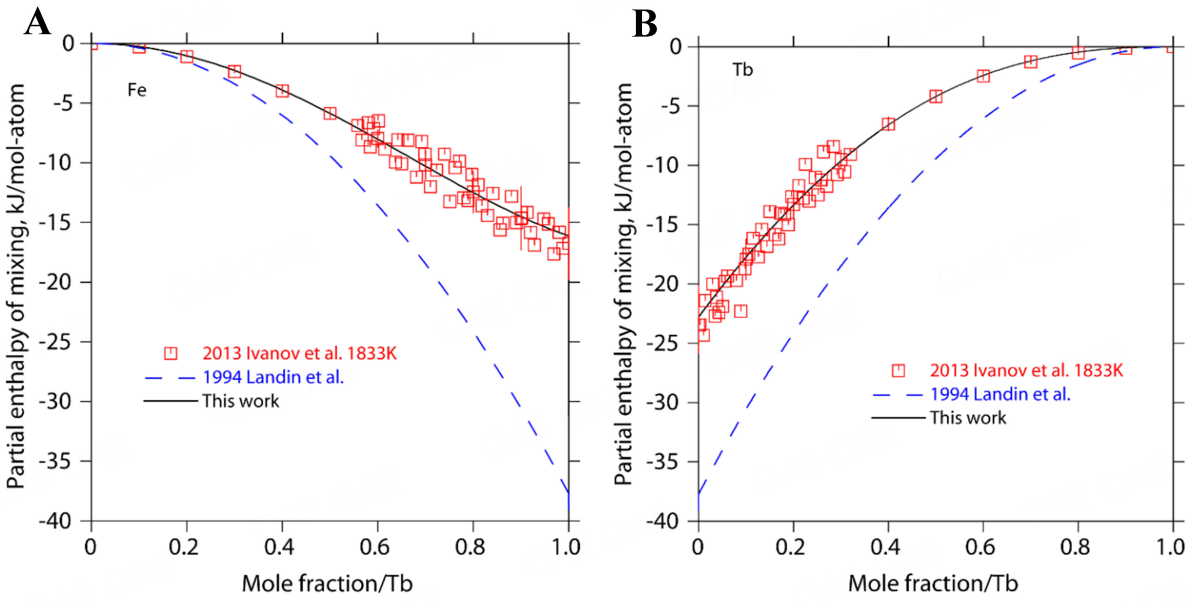

Figure 3. Calculated partial enthalpy of Fe (A) and Tb (B) in liquid Fe-Tb alloys at 1,833 K with the calculation[104] and the experimental data[53].

Figure 19 shows the presently calculated heat capacity of $Fe_{17}Lu_2$ along with the measured results[113] and the calculations[90]. The calculated heat capacity of $Fe_{17}Lu_2$ agrees with the results[113], while the results calculated by Kardellass *et al.* are significantly different[90]. Figure 20 is the calculated the heat capacity, the entropy of formation, and the enthalpy difference of Fe_2Lu with the measured results[101] and the calculations[90]. Comparing with the previous calculations[90], the heat capacity of Fe_2Lu calculated in this study is in better accordance with the results[101].

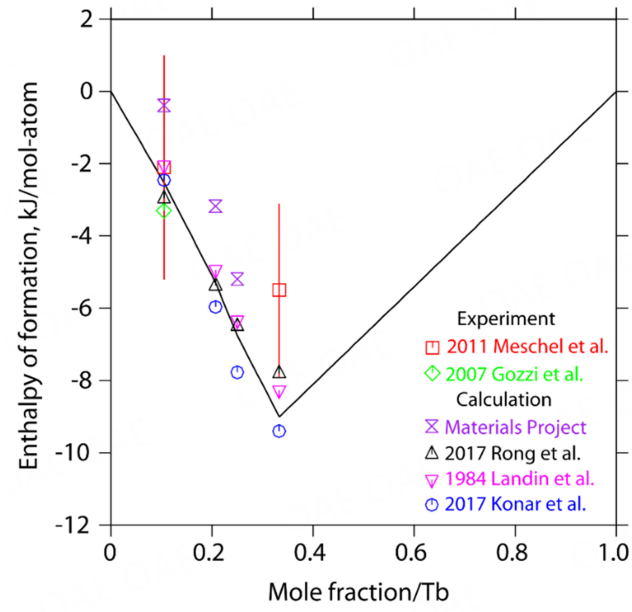

Figure 4. Calculated enthalpies of formation of the Fe-Tb intermetallic compounds at 298 K with the experimental results[54,102] and the calculations[19,27,104,140].

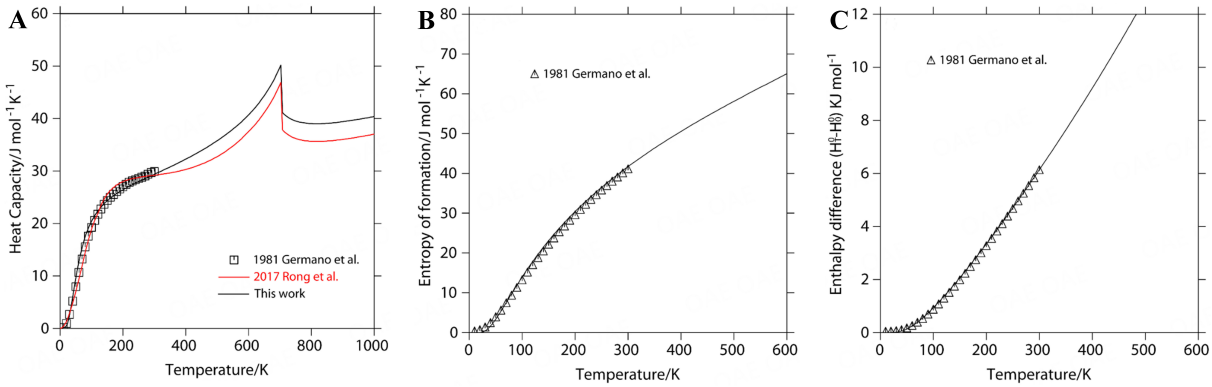

Figure 5. The calculated (A) heat capacity, (B) the entropy of formation, and (C) the enthalpy difference $(H_T^0 - H_0^0)$ of Fe_2Tb with the calculations[27] and the experimental data[101].

Fe-Y

Figure 21 shows the calculated Fe-Y binary system along with the earlier calculations[127,131-133] and the experimental results[115]. It is evident in Figure 21A that the previous calculations[127] show that $Fe_{23}Y_6$ and Fe_2Y are not stable at low temperature, while four intermetallic compounds (including $Fe_{23}Y_6$ and Fe_2Y) are stable down to room temperature in this study. As displayed in Figure 21B, the present calculations agree with the measured results[115]. Table 10 summarizes the present calculations of the invariant reactions together with the calculations[127,131-133], and the optimized parameters in this work are shown in Table 5. Four eutectic reactions, L ↔ $Fe_{17}Y_2$ + fcc-Fe, L ↔ $Fe_{17}Y_2$ + $Fe_{23}Y_6$, L ↔ $Fe_{23}Y_6$ + Fe_3Y, and L ↔ Fe_2Y + hcp-Y, are calculated to be 1,647.3 K and 8.8 at.% Y, 1,602.7 K and 19.7 at.% Y, 1,602.4 K and 22.1 at.% Y, and 1,163.5 K and 65.6 at.% Y, respectively. The temperatures of the congruent reaction of $Fe_{17}Y_2$, $Fe_{23}Y_6$, and Fe_3Y are calculated to be 1,620.1 K, 1,603.0 K, and 1,605.5 K, respectively, while two peritectic reactions, L + Fe_3Y ↔ Fe_2Y and L + bcc-Fe ↔ fcc-Fe, are calculated to be 1,666.8 K and 1,163.5 K, respectively, which

Table 10. . Invariant reactions of the Fe-Y binary system

Reactions	Reaction type	Temperature (K)	Composition (x_Y^L)	Reference
bcc(δ-Fe) ↔ fcc(γ-Fe) + L	Metatectic	1673±25	—	[115] (exp.)
		1667.0	0.058	[127] (cal.)
		1665.0	0.072	[132] (cal.)
		1725.0	0.039	[19] (cal.)
		1663.0	0.048	[131] (PTD) (cal.)
		1664.0	0.048	[131] (ETD) (cal.)
		1660.0	0.060	[133] (cal.)
		1665.8	0.077	This work(cal.)
fcc(γ-Fe) ↔ bcc(α-Fe) + $Fe_{17}Y_2$	Eutectoid	1185.0	—	[115] (exp)
		1185.0	—	[132]
		1185.0	—	[133]
		1185.0	—	[131] (PTD) (cal.)
		1185.0	—	[131] (ETD) (cal.)
		1184.8	—	This work
L ↔ $Fe_{17}Y_2$+ fcc(γ-Fe)	Eutectic	1623±25	0.082	[115] (exp.)
		1623.0	0.074	[127] (cal.)
		1641.0	0.084	[132] (cal.)
		1657.0	0.069	[19] (cal.)
		1633.0	0.056	[131] (PTD) (cal.)
		1663.0	0.072	[131] (ETD) (cal.)
		1635.0	0.070	[133] (cal.)
		1647.3	0.088	This work(cal.)
L↔ $Fe_{17}Y_2$	Congruent	1673±25	0.105	[115] (exp.)
		1673.0	0.105	[127] (cal.)
		1644.0	0.105	[132] (cal.)
		1679.0	0.105	[19] (cal.)
		1676.0	0.105	[131] (PTD) (cal.)
		1672.0	0.105	[131] (ETD) (cal.)
		1650.0	0.105	[133] (cal.)
		1650.1	0.105	This work(cal.)
L ↔ $Fe_{17}Y_2$ + $Fe_{23}Y_6$	Eutectic	~1553.0	0.129	[115] (exp.)
		1553.0	0.164	[127] (cal.)
		1605.0	0.197	[132] (cal.)
		1645.0	0.159	[19] (cal.)
		1605.0	0.182	[131] (PTD) (cal.)
		1638.0	0.179	[131] (ETD) (cal.)
		1613.0	0.173	[133] (cal.)
		1602.7	0.197	This work(cal.)
L ↔ $Fe_{23}Y_6$	Congruent	~1573.0	—	[115] (exp.)
		1606.0	0.201	[132] (cal.)
		1667.0	0.207	[19] (cal.)
		1606.0	0.207	[131] (PTD) (cal.)
		1641.0	0.207	[131] (ETD) (cal.)
		1623.0	0.207	[133] (cal.)
		1603.0	0.207	This work(cal.)
L ↔ $Fe_{23}Y_6$ + Fe_3Y	Eutectic	~1523.0	0.237	[115] (exp.)
		1573.0	0.186	[127] (cal.)
		1604.0	0.237	[132] (cal.)
		1667.0	0.210	[19] (cal.)
		1605.0	0.207	[131] (PTD) (cal.)
		1640.0	0.216	[131] (ETD) (cal.)
		1619.0	0.207	[133] (cal.)
		1602.4	0.221	This work(cal.)
L ↔ Fe_3Y	Congruent	~1608.0	0.250	[115] (exp.)
		1623.0	0.250	[127] (cal.)
		1605.0	0.250	[132] (cal.)
		1681.0	0.250	[19] (cal.)
		1623.0	0.250	[131] (PTD) (cal.)
		1647.0	0.250	[131] (ETD) (cal.)
		1621.0	0.250	[133] (cal.)
		1605.5	0.250	This work(cal.)
L + Fe_3Y ↔ Fe_2Y	Peritectic	1398±25	~0.424	[115] (exp.)
		1398.0	0.421	[127] (cal.)
		1396.0	0.525	[132] (cal.)
		1397.0	0.475	[19] (cal.)
		1409.0	0.443	[131] (PTD) (cal.)
		1397.0	0.482	[131] (ETD) (cal.)

		1416.0	0.467	[133] (cal.)
		1421.0	0.490	This work(cal.)
L ↔ Fe_2Y + hcp-Y	Eutectic	1173±10	~0.660	[115] (exp.)
		1173.0	0.651	[127] (cal.)
		1201.0	0.661	[132] (cal.)
		1156.0	0.601	[19] (cal.)
		1146.0	0.612	[131] (PTD) (cal.)
		1118.0	0.637	[131] (ETD) (cal.)
		1120.0	0.640	[133] (cal.)
		1163.5	0.656	This work(cal.)
L + bcc-Y ↔ hcp-Y	Peritectic	1758.0	—	[115] (exp.)
		1752.0	0.979	[127] (cal.)
		1756.0	0.983	[132] (cal.)
		1752.0	0.978	[19] (cal.)
		1750.0	0.979	[131] (PTD) (cal.)
		1749.0	0.976	[131] (ETD) (cal.)
		1754.0	0.980	[133] (cal.)
		1757.1	0.981	This work(cal.)

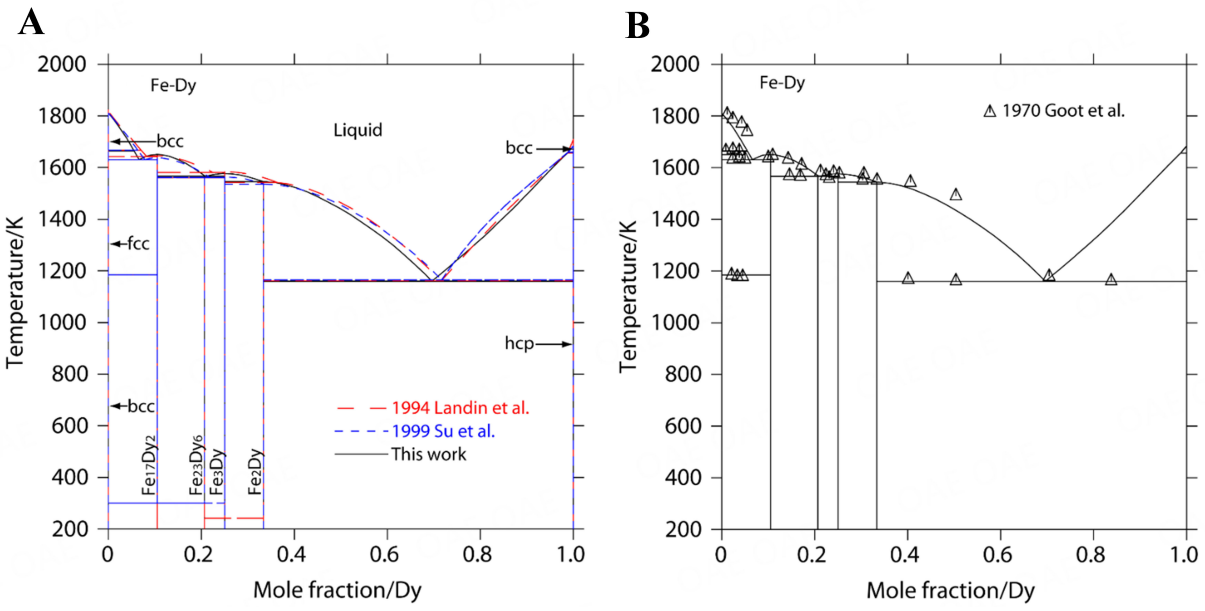

Figure 6. Calculated Fe-Dy binary phase diagram with (A) the calculations[104,105] and (B) the experimental data[96].

are in accordance with the results[115].

As shown in Figure 22, the enthalpy of mixing of liquid Fe-Y alloys is calculated at 1,873 K and compared with the determined results[121] and the calculations[127,131-133]. The calculations[127,131] are a visible deviation from the experimental results[121], while the present calculations are in accordance with the results[121]. Figure 23 depicts the partial enthalpy of mixing of Fe and Y calculated by this study at 1,873 K with the measured data[121,122] and the calculations[127,131-133]. It was found that the present calculations are accordant with the results[121], while the previous calculations[127,131-133] show obvious differences. Figure 24 shows the calculated enthalpy of formation of the Fe-Y intermetallic compounds at 298 K with the measured data[123] and the calculations[127,131-133]. The enthalpies of formation of $Fe_{17}Y_2$, $Fe_{23}Y_6$, Fe_3Y, and Fe_2Y are calculated to be -2.994, -5.061, -6.417, and -7.446 kJ/mol-atom, respectively. It was found that the calculated enthalpy of formation of Fe_2Y is the most negative. Generally, the enthalpy of formation of Fe_2RE is the most negative in Fe-RE binary systems. It is still necessary to measure the enthalpy of formation of the Fe-Y compounds in

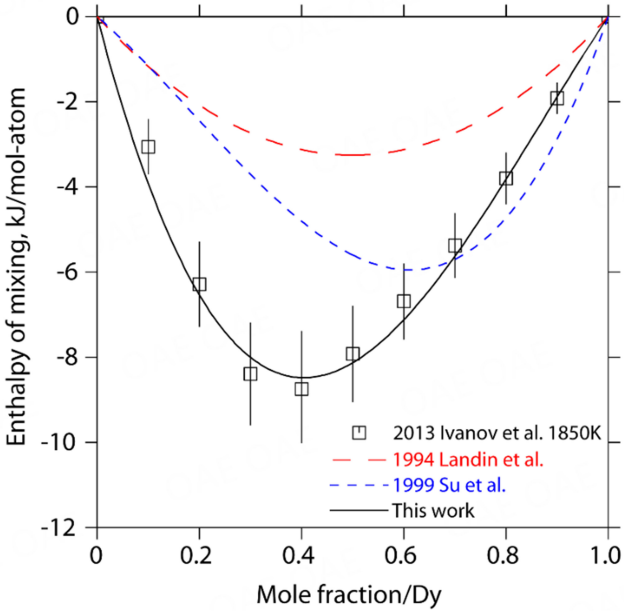

Figure 7. The calculated enthalpy of mixing of liquid Fe-Dy alloys at 1,850 K with the experimental results[53] and the calculations[104,105].

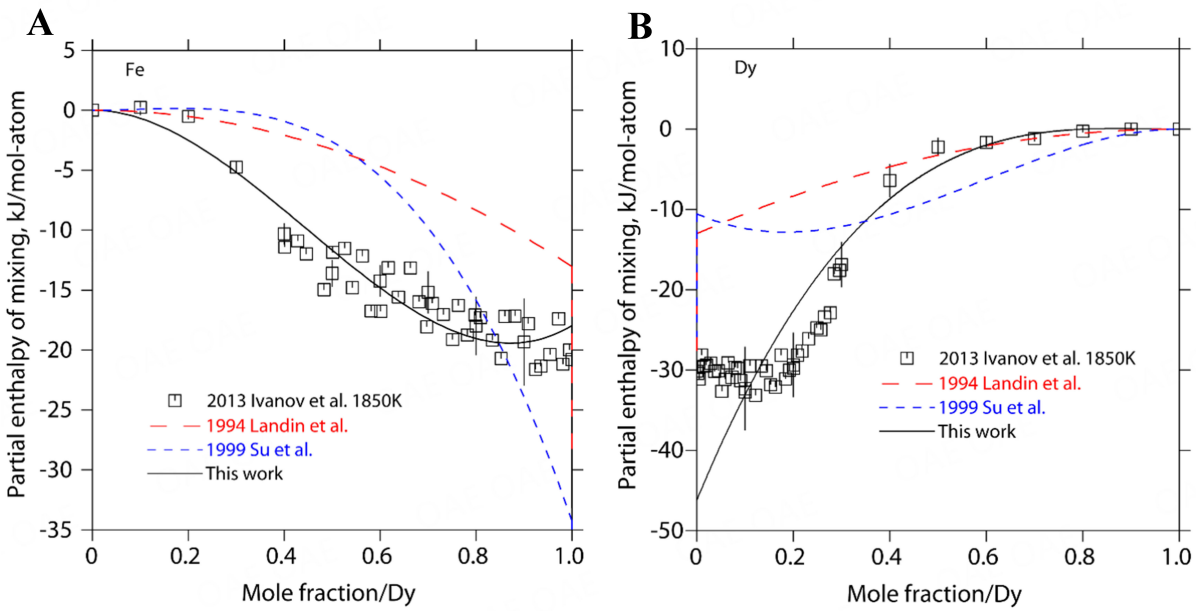

Figure 8. Calculated partial enthalpy of mixing of Fe (A) and Dy (B) in liquid Fe-Dy alloys at 1,850 K with the experimental data[53] and the calculations[104,105].

further experiments.

Figure 25 depicts the calculated heat capacity of $Fe_{17}Y_2$ with the reported results[125]. The calculated heat capacity of $Fe_{17}Y_2$ at low temperature (below 298 K) is accordant well with the results[125], while Konor *et al.* did not consider the experimental heat capacity of $Fe_{17}Y_2$[19]. Figure 26 shows the calculated activities of Fe and Y at 1,473 K and 1,573 K with the determined results[126]. It is clear that the calculated activities of Fe

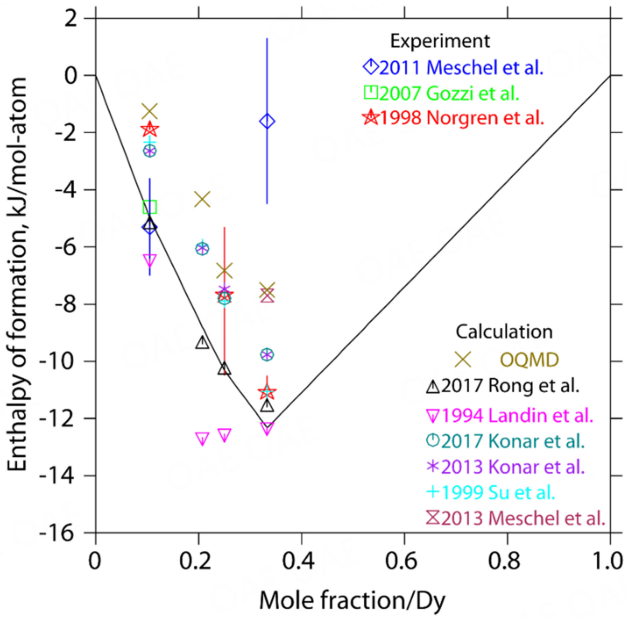

Figure 9. Calculated enthalpy of formation of the Fe-Dy intermetallic compounds at 298 K with the experimental data[54,102,103] and the calculations[19,27,44,83,104,105,141].

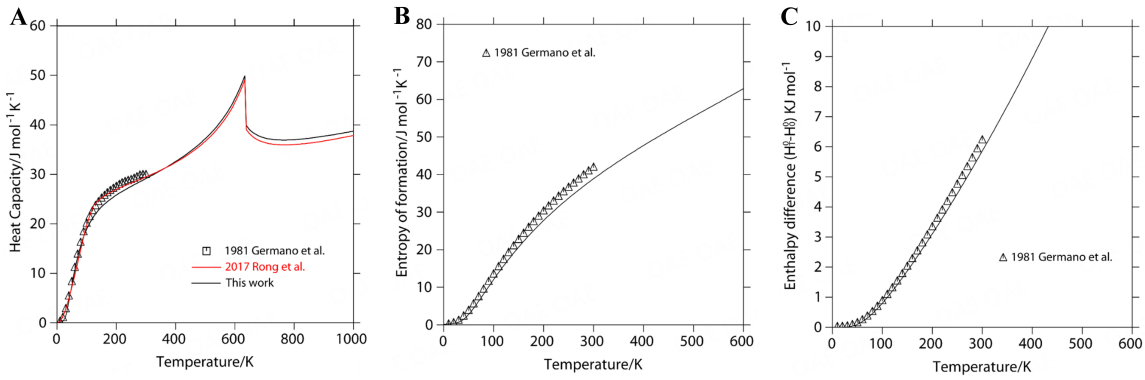

Figure 10. The calculated (A) heat capacity, (B) the entropy of formation, and (C) the enthalpy difference $(H_T^0 - H_0^0)$ of Fe_2Dy with the experimental data[101] and the calculations[27].

and Y in the Fe-rich region are much better consistent with the reported results[126] than those of Fe and Y in the Y-rich region, which could be resulted from the oxidation of Fe-Y alloys.

DISCUSSION

RE metals show similar physicochemical properties because of their unique and similar electronic configurations. The alloys made of RE metals and transition metals are expected to show a trend in phase equilibria and thermodynamic properties of the RE-TM (transition metals) binary systems as the RE atomic number increases. Our previous work[25,26,28,29] shows that the calculated phase equilibria and thermodynamic properties of some Fe-RE binary systems are accordant well with the experimental data, as displayed in Figure 27. In the following section, phase equilibria and thermodynamic properties of thirteen Fe-RE binary systems were analyzed systematically.

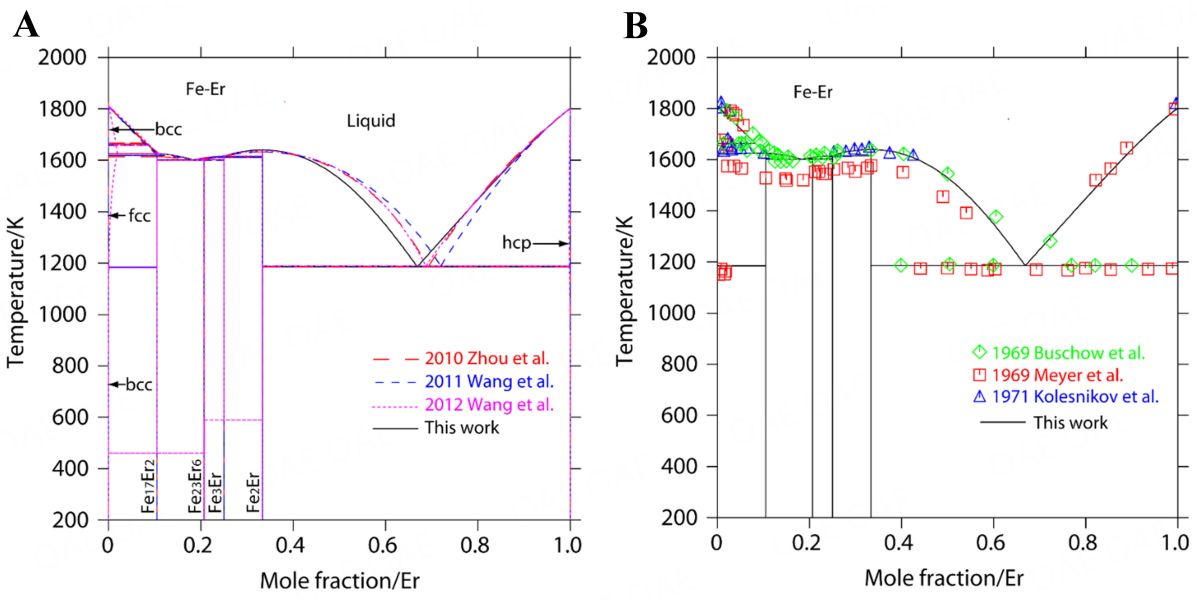

Figure 11. Calculated Fe-Er binary phase diagram with (A) the calculations[110-112] and (B) the experimental data[106-108].

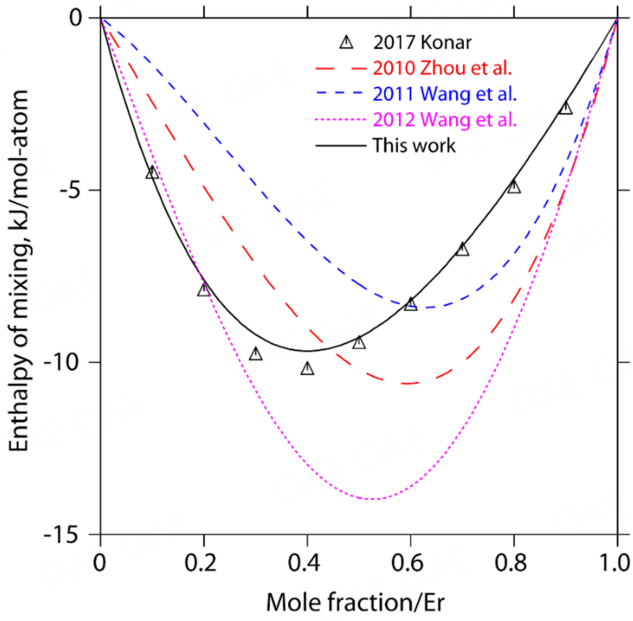

Figure 12. The calculated enthalpy of mixing of liquid Fe-Er alloys at 1,833 K with the calculations[19,110-112].

Phase equilibria

In Figure 28, the Fe-RE binary phase diagrams demonstrate that the number of stable intermetallic compounds in generally increases from 0 to 4 as the RE atomic number increases. With the increasing of the RE atomic number, $Fe_{17}RE_2$, $Fe_{17}RE_5$, Fe_3RE, Fe_2RE, and $Fe_{23}RE_6$ appear successively in the Fe-RE (RE = Pr, Nd, Sm, Gd, Tb, Dy, Ho, Er, Tm, Lu, and Y) binary phase diagrams, as given in Table 11. Notably, $Fe_{17}RE_2$, $Fe_{23}RE_6$, Fe_3RE, and Fe_2RE are stable in the Fe-RE (RE = Gd, Tb, Dy, Ho, Er, Tm, Lu, and Y) binary systems. However, $Fe_{23}RE_6$ does not exist in the Fe-RE (RE = La, Ce, Pr, Nd, and Sm) binary systems. In addition,

Table 11. Temperatures of formation reaction for Fe-RE intermetallic compounds

Systems	$Fe_{17}RE_2$	$Fe_{23}RE_6$	$Fe_{17}RE_5$	Fe_3RE	Fe_2RE
Fe-La	—	—	—	—	—
Fe-Ce	1344.6^P	—	—	—	1205.6^P
Fe-Pr	1383.0^P	—	—	—	—
Fe-Nd	1490.0^P	—	1071.0^P	—	—
Fe-Sm	1557.0^P	—	—	1287.0^P	1174.0^P
Fe-Gd	1604.0^P	1556.0^P	—	1429.0^P	1354.5^P
Fe-Tb	1587.5^C	1561.1^C	—	1486.0^P	1462.7^P
Fe-Dy	1651.0^C	1567.4^P	—	1576.4^C	1545.5^P
Fe-Ho	1615.6^C	1605.2^C	—	1567.6^P	1565.0^C
Fe-Er	1625.1^P	1602.7^P	—	1615.0^P	1640.4^C
Fe-Tm	1573.4^P	1544.6^P	—	1552.5^P	1572.6^C
Fe-Lu	1590.1^P	1560.9^P	—	1580.4^P	1619.6^C
Fe-Y	1650.1^C	1603.0^C	—	1605.5^C	1421.0^P

C: Congruent; P: peritectic.

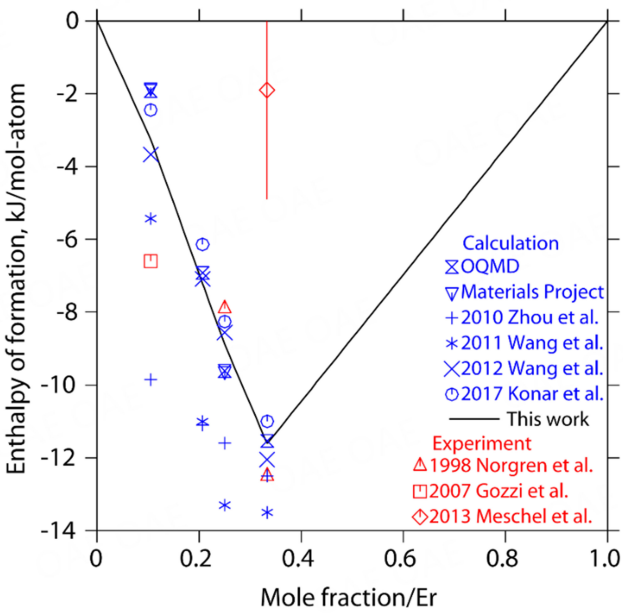

Figure 13. Calculated enthalpies of formation of the Fe-Er intermetallic compounds at 298 K with the experimental data[44,54,103] and the calculations[19,110-112,140,141].

$Fe_{17}RE_5$ only exists in the Fe-Nd binary system, and $Fe_{17}RE_2$ is stable in the Fe-RE (apart from Fe-La) binary systems.

The types and temperatures of the invariant reactions for the formation of the Fe-RE (e.g., $Fe_{17}RE_2$, Fe_3RE, Fe_2RE, and $Fe_{23}RE_6$) intermetallic compounds are demonstrated in Figure 28 and Table 11. As can be easily seen in the Fe-RE (RE = Ce, Pr, Nd, Sm, Gd, Er, Tm, and Lu) binary systems, $Fe_{17}RE_2$ is produced through the peritectic reaction, but by the congruent reaction in the Fe-RE (RE = Tb, Dy, Ho, and Y) binary systems; $Fe_{23}RE_6$ is produced by the congruent reaction in the Fe-RE (RE = Tb, Ho, and Y) binary systems, but by peritectic reaction in the Fe-RE (RE = Gd, Dy, Er, Tm, Lu, and Y) binary systems; Fe_3RE is produced by the

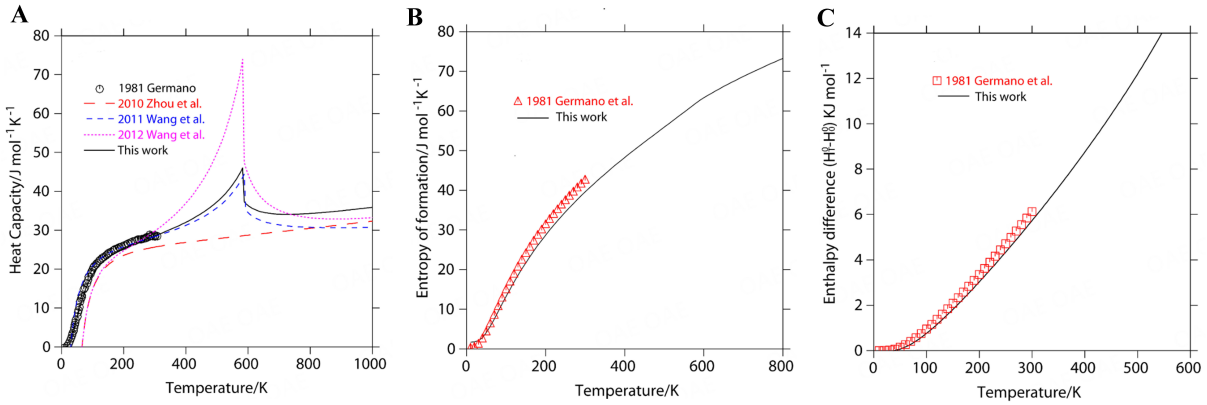

Figure 14. The calculated (A) heat capacity, (B) the entropy of formation and (C) the enthalpy difference $(H_T^0 - H_0^0)$ of Fe Er with the experimental data[101] and the calculated results[110-112].

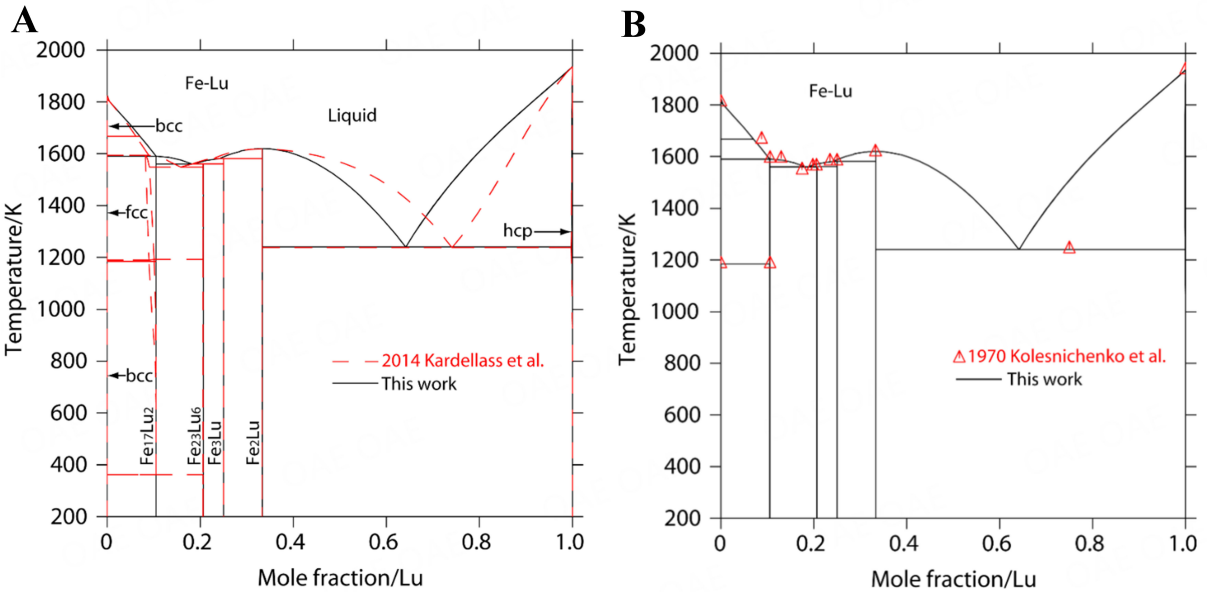

Figure 15. Calculated Fe-Lu binary phase diagram with (A) the calculations[90] and (B) the experimental data[88].

congruent reaction in the Fe-Dy and Fe-Y binary systems, but by the peritectic reaction in the Fe-RE (RE = Sm, Gd, Tb, Ho, Er, Tm, and Lu) binary systems; Fe_2RE is produced through the peritectic reaction in the Fe-RE (RE = Ce, Sm, Gd, Tb, Dy, and Y) binary systems, but through the congruent reaction in the Fe-RE (RE=Ho, Er, Tm, and Lu) binary systems. The melting points of RE metals increase gradually with the RE atomic number increases, and the reaction temperatures and types for the intermetallic compounds show a similar trend. In general, the reaction temperatures of $Fe_{17}RE_2$, Fe_3RE, and Fe_2RE in the Fe-RE (RE = Ce, Pr, Nd, Sm, Gd, Tb, Dy, Ho, Er, Tm, and Lu) binary systems become higher with the increase of the RE atomic number. The reaction temperature of $Fe_{23}RE_6$ also displays this trend in the Fe-RE (RE = Gd, Tb, Dy, Ho, and Er) binary systems, but it is not clear in the Fe-Tm and Fe-Lu binary systems.

Thermodynamic properties

Figure 29 depicts the calculated enthalpy of mixing of liquid Fe-RE alloys. It was found that the enthalpy of

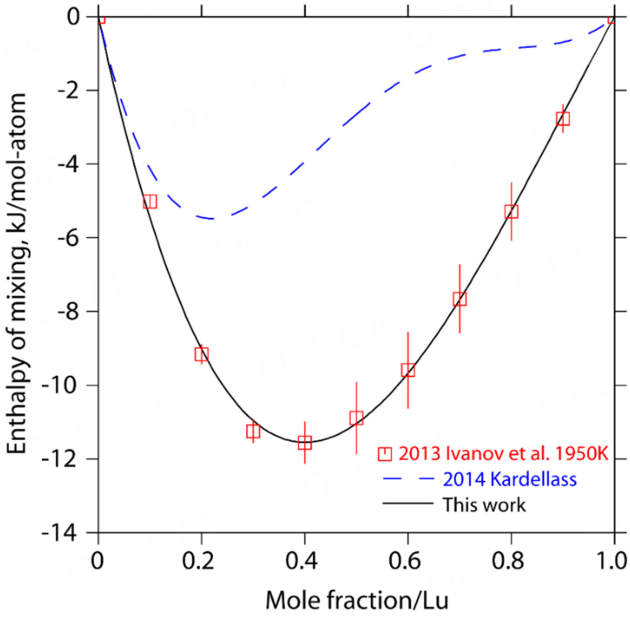

Figure 16. The calculated enthalpy of mixing of liquid Fe-Lu alloys at 1,950 K with the experimental data[53] and the calculations[90].

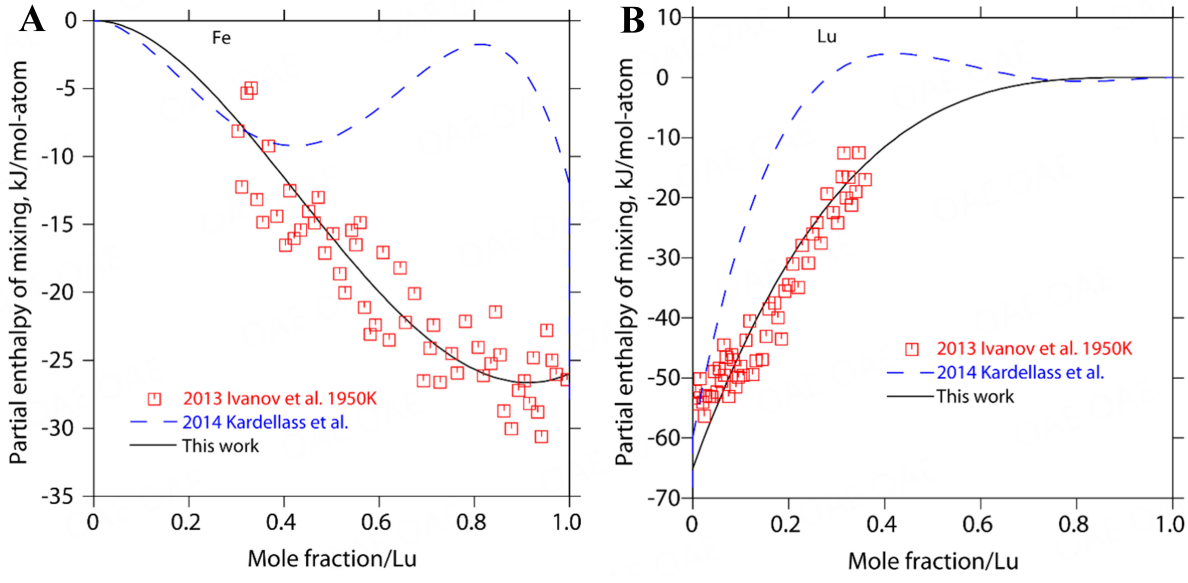

Figure 17. Calculated partial enthalpy of Fe (A) and Lu (B) in liquid Fe-Lu alloys at 1,950 K with the experimental data[53] and the calculations[90].

mixing of liquid Fe-La alloys is positive, while that of liquid Fe-Pr alloys is positive and negative over different composition regions. Meanwhile, the calculated enthalpy of mixing in liquid Fe-RE (RE = Ce, Nd, Sm, Gd, Tb, Dy, Ho, Er, Tm, Lu, and Y) alloys is all negative. The minimum enthalpy of mixing of liquid Fe-RE (RE = Ce, Nd, Sm, Gd, Tb, Dy, Ho, Er, Tm, and Lu) alloys is located in the composition range of 30 at.%-50 at.% RE. In general, the enthalpy of mixing of liquid Fe-RE (apart from Fe-Ce and Fe-Y) alloys is calculated and displayed a tendency that the higher the RE atomic number, the more negative the enthalpy of mixing. The similar irregularities of the enthalpy of mixing of liquid Fe-Ce and Fe-Y alloys in the Fe-RE

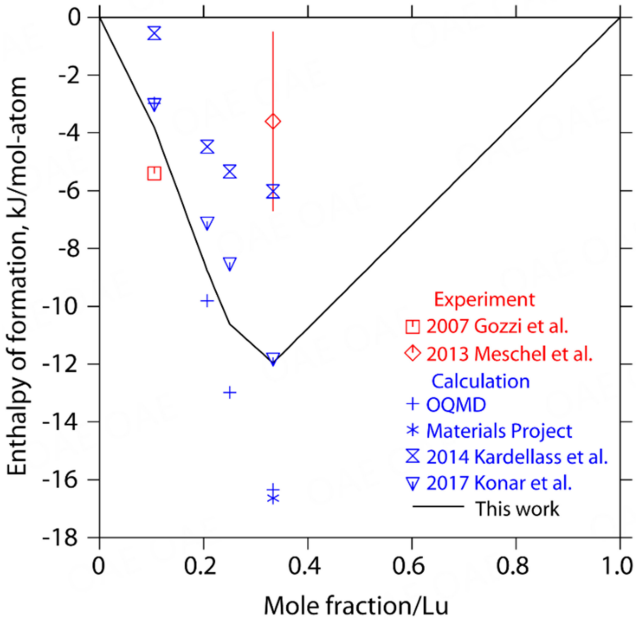

Figure 18. Calculated enthalpies of formation of the Fe-Lu intermetallic compounds at 298 K with the experimental data[44,54] and the calculations[19,90,140,141].

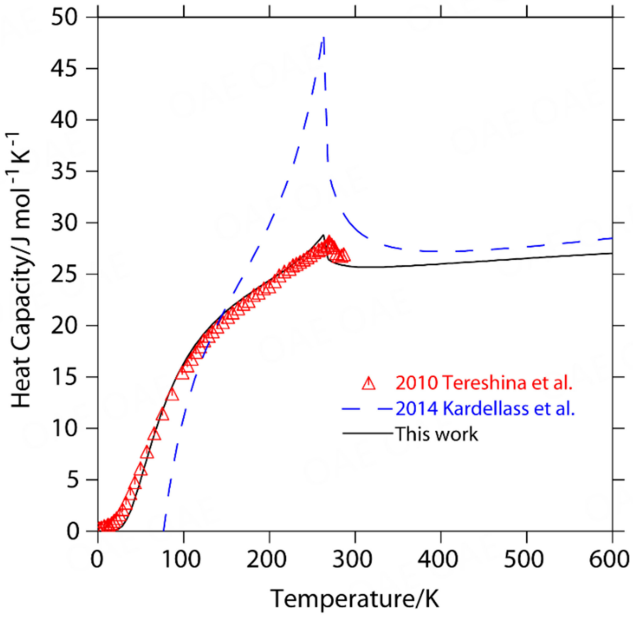

Figure 19. Calculated heat capacity of $Fe_{17}Lu_2$ with the experimental data[113] and the calculations[90].

binary systems were also observed in the B-RE[24] and Ni-RE[139] binary systems. Due to a lack of the experimental data on the enthalpy of mixing of liquid Fe-Er alloys, the thermodynamic calculation of the Fe-Er binary system was performed by taking this regular trend into account in the present study.

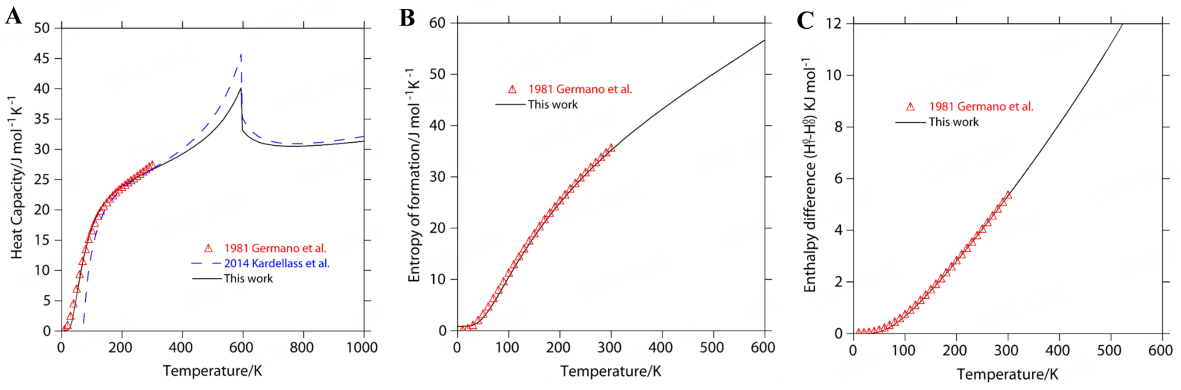

Figure 20. The calculated (A) heat capacity, (B) the entropy of formation, and (C) the enthalpy difference $(H_T^0 - H_0^0)$ of Fe_2Lu with the experimental data[101] and the calculations[90].

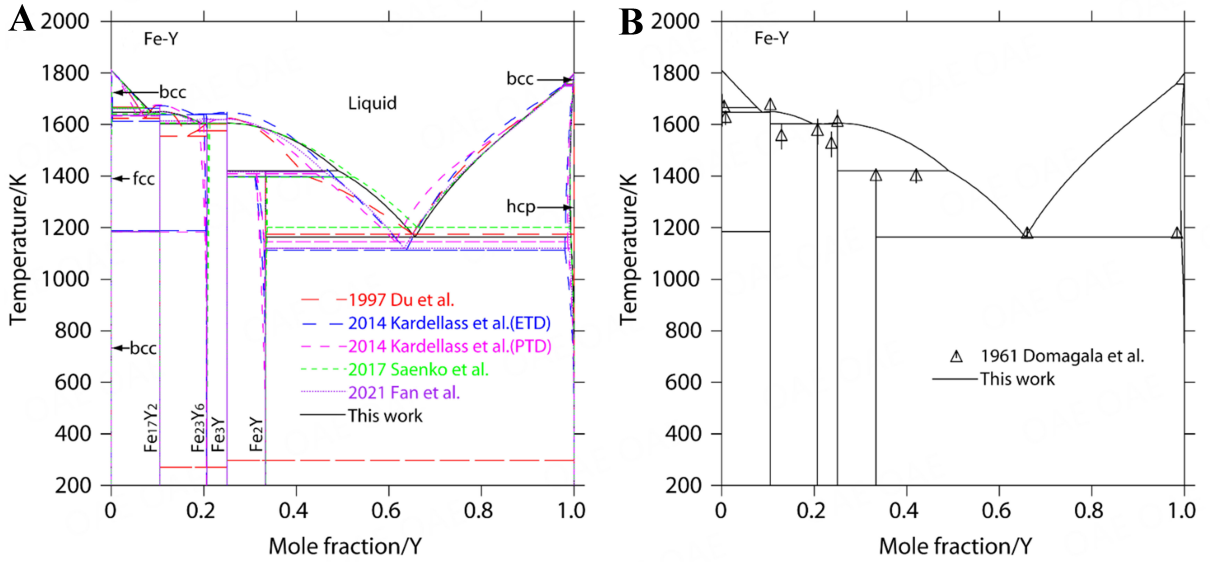

Figure 21. Calculated Fe-Y binary phase diagram with (A) the calculations[127,131-133] and (B) the experimental data[115].

Figure 30 displays the calculated enthalpy of formation of the Fe-RE intermetallic compounds at 298 K (e.g., $Fe_{17}RE_2$, $Fe_{17}RE_5$, Fe_3RE, Fe_2RE, and $Fe_{23}RE_6$). The enthalpy of formation Fe_2RE is the most negative and shows a trend that the enthalpy of formation of Fe_2RE becomes increasingly negative with the RE atomic number increases in the Fe-RE (apart from Fe-Y, Fe-Gd, and Fe-Dy) binary systems. It is noted that the enthalpy of formation of the Fe-Gd intermetallic compounds is more negative than those of the Fe-Tb intermetallic compounds. In particular, the enthalpy of formation of the Fe-Y intermetallic compounds is between that of the Fe-Sm intermetallic compounds and that of the Fe-Gd intermetallic compounds. There are similar irregularities that also appear in the RE-B[24], RE-Mn[137,138], and RE-Ni[139] binary systems. Generally, the enthalpy of formation of the Fe-RE intermetallic compounds become increasingly negative with an increasing of the RE atomic number. It indicates stronger bond in Fe-RE (apart from Fe-Y) binary systems as a consequence of the reducing atomic radius with the increasing of the RE atomic number.

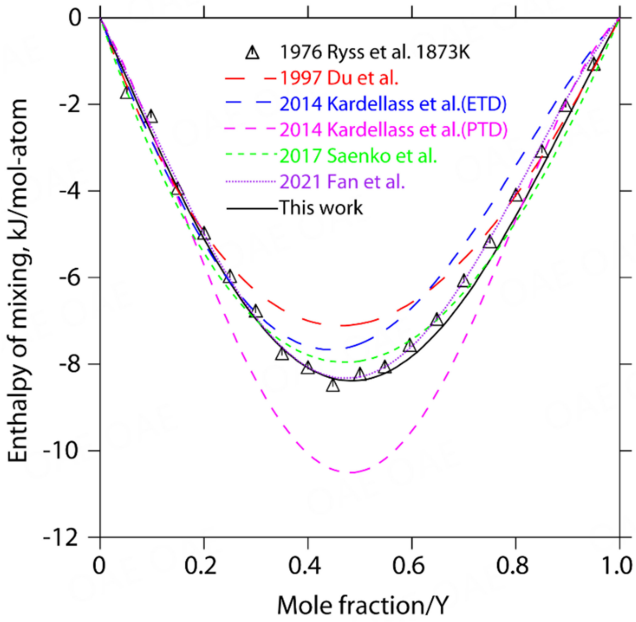

Figure 22. The calculated enthalpy of mixing of liquid Fe-Y alloys at 1,873 K with the experimental data[121] and the calculations[127,131-133].

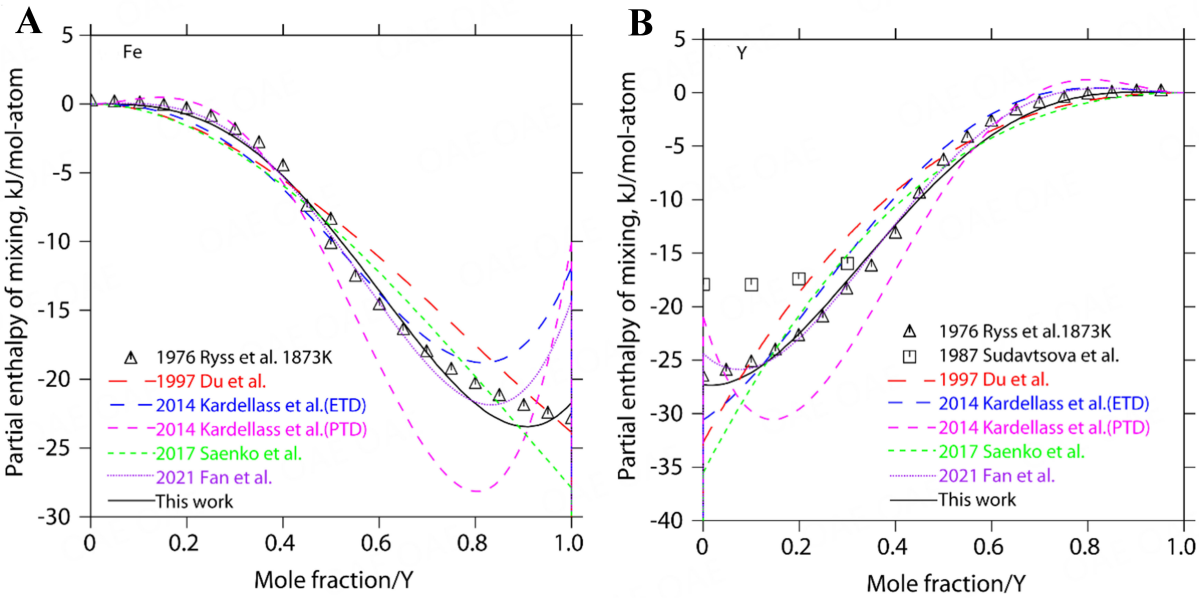

Figure 23. Calculated partial enthalpy of (A) Fe and (B) Y in liquid Fe-Y alloys at 1,873 K with the experimental data[121,122] and the calculations[127,131-133].

SUMMARY

Three Fe-Er, Fe-Lu, and Fe-Y binary systems were reassessed through the CALPHAD method in the present work according to the reliable experimental results and the earlier calculations in the literature. An improvement to our previous assessments of the Fe-Tb and Fe-Dy binary systems was obtained by revising the expressions of the Gibbs energies of Fe_2Tb and Fe_2Dy and thus eliminating the artificial break in their heat capacity curves that appears in the earlier assessments. A set of available thermodynamic parameters

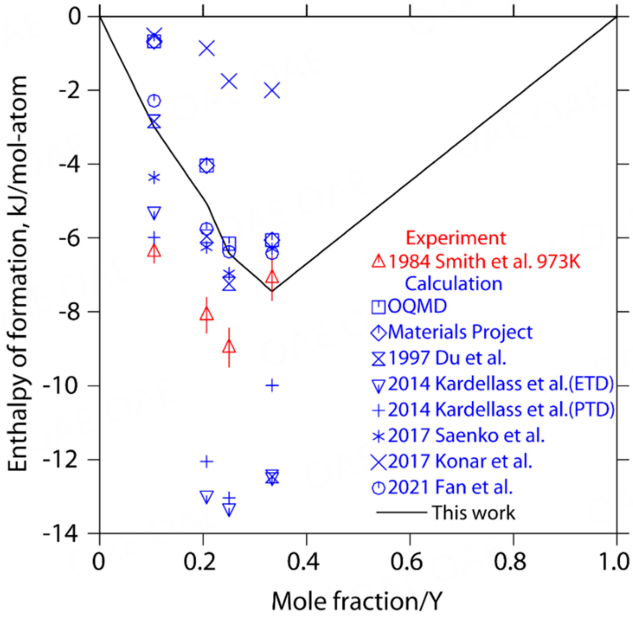

Figure 24. Calculated enthalpies of formation of the Fe-Y intermetallic compounds at 298 K with the experimental data[123] and the calculations[127,131-133].

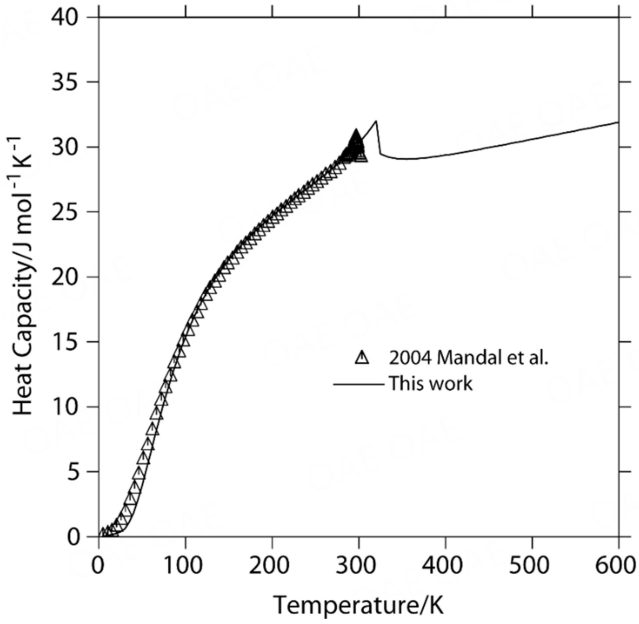

Figure 25. The calculated heat capacity of $Fe_{17}Y_2$ with the experimental data[125].

for describing the Gibbs energies of all the phases in the Fe-RE (RE = Tb, Dy, Er, Lu, and Y) binary systems are used to calculate thermodynamic properties and phase equilibria of these five binary systems accurately.

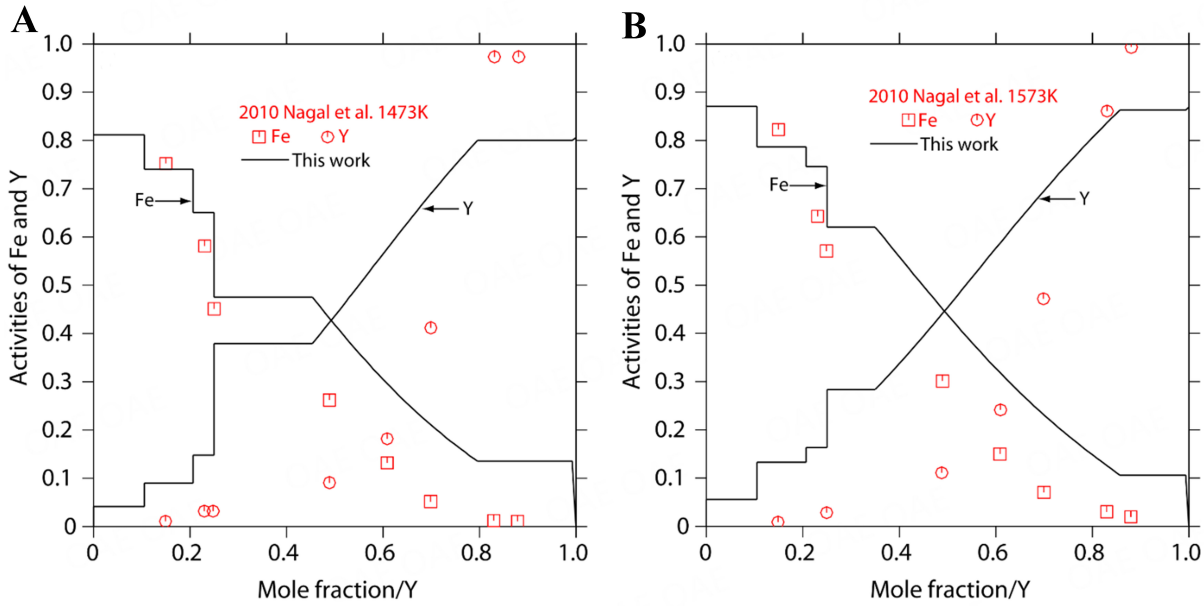

Figure 26. The calculated activities of Fe and Y at (A) 1,473 K and (B) 1,573 K with the experimental data[126].

Combining with the present assessments of the Fe-RE (RE = Tb, Dy, Er, Lu, and Y) binary systems and the previous calculations of the Fe-RE (RE = La, Ce, Pr, Nd, Sm, Gd, Ho, and Tm) binary systems, phase equilibria, and thermodynamic characteristics of thirteen Fe-RE binary systems were discussed systematically. A tend was demonstrated for the change of phase equilibria and thermodynamic properties of the Fe-RE alloys with the RE atomic number. Generally, as the increase of the RE atomic number, the formation temperatures of the Fe-RE intermetallic compounds increase gradually, and the enthalpy of mixing of liquid Fe-RE (apart from Fe-Ce and Fe-Y) alloys as same as the enthalpy of formation of the Fe-RE (apart from Fe-Y, Fe-Ce, Fe-Gd, Fe-Dy) intermetallic compounds become increasingly negative. In conclusion, the self-consistent set of thermodynamic parameters of the Fe-RE binary systems was finally obtained in this study, which would provide a solid basis for developing a thermodynamic database of Fe-RE-based alloy systems.

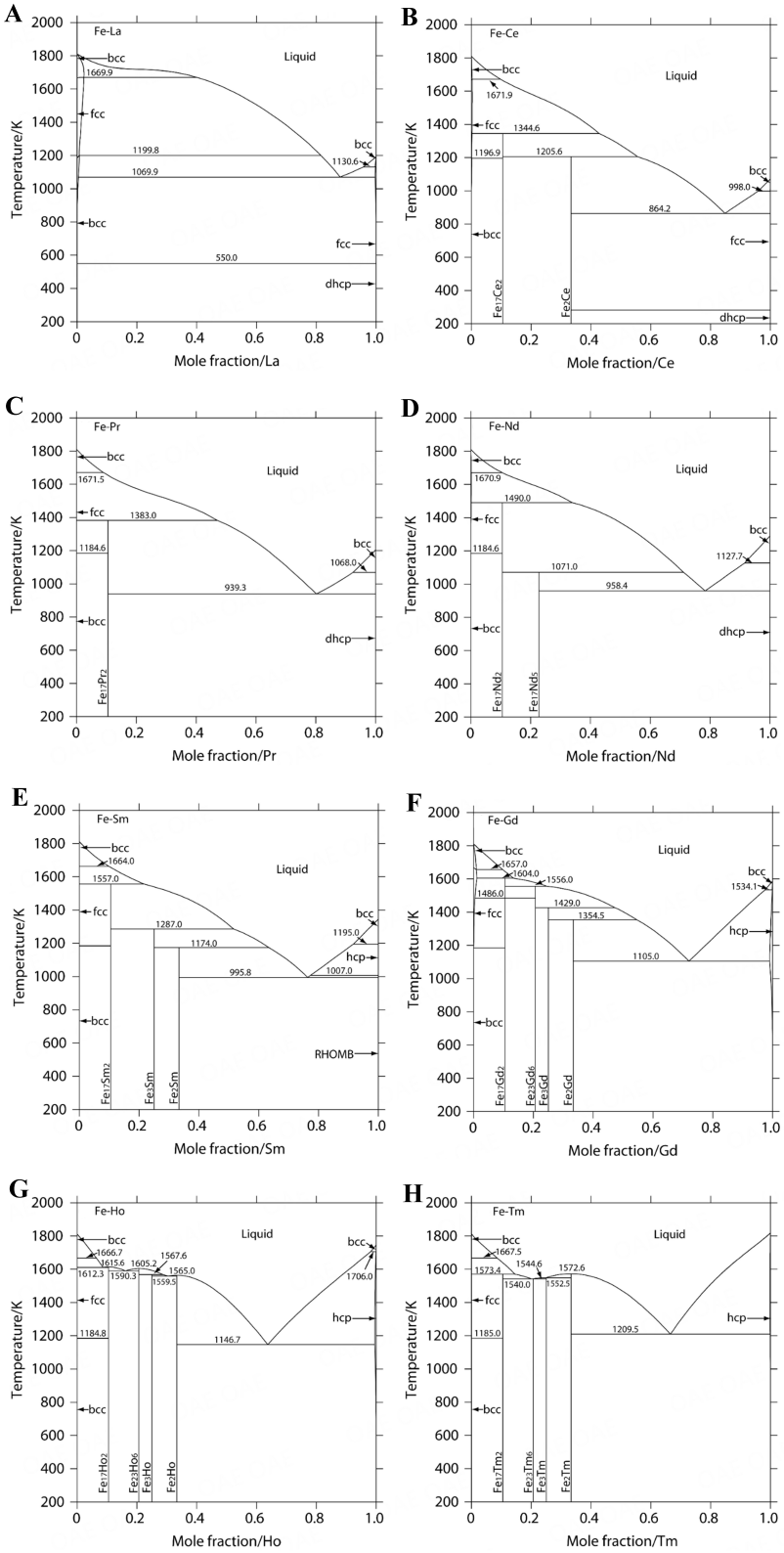

Figure 27. The calculated Fe-RE binary phase diagrams. (A) Fe-La[29]; (B) Fe-Ce[29]; (C) Fe-Pr[25]; (D) Fe-Nd[25]; (E) Fe-Sm[26]; (F) Fe-Gd[26]; (G) Fe-Ho[28]; (H) Fe-Tm[28]

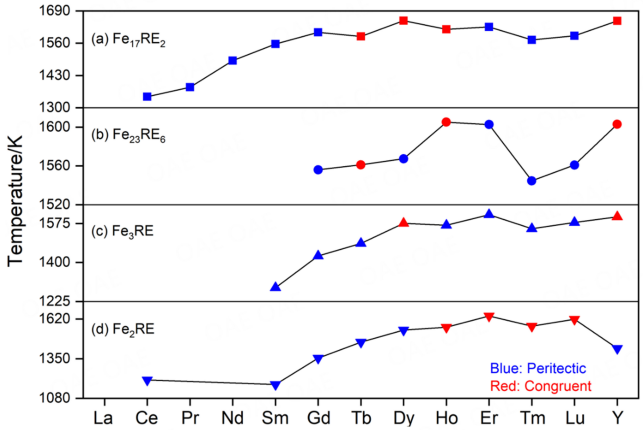

Figure 28. The reaction temperatures of the Fe-RE (RE = La, Ce, Pr, Nd, Sm, Gd, Tb, Dy, Ho, Er, Tm, Lu and Y) intermetallic compounds. (A) $Fe_{17}RE_2$; (B) $Fe_{23}RE_6$; (C) Fe_3RE; (d) Fe_2RE.

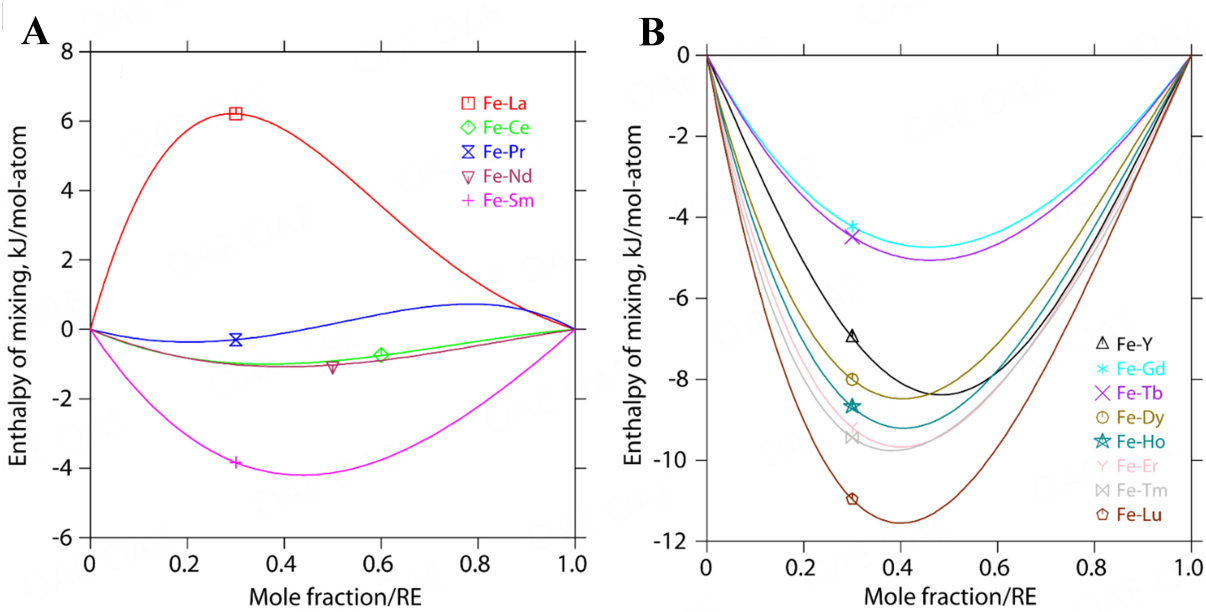

Figure 29. The calculated enthalpies of mixing of liquid Fe-RE (RE = La, Ce, Pr, Nd, Sm, Gd, Tb, Dy, Ho, Er, Tm, Lu and Y) alloys.

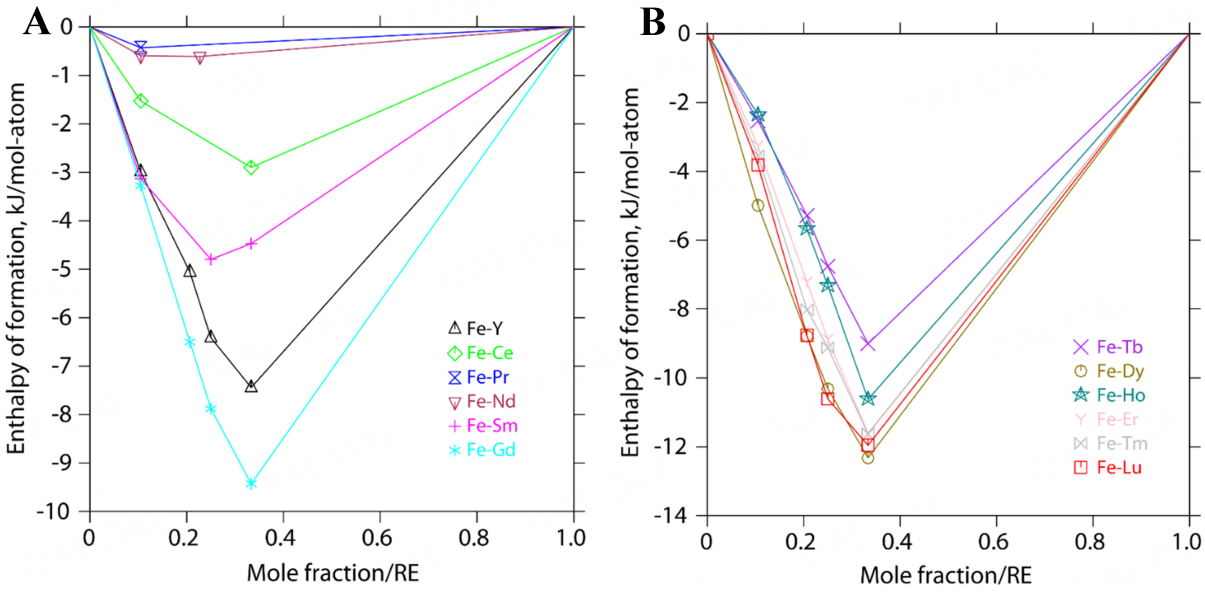

Figure 30. The calculated enthalpies of formation of the Fe-RE (RE = La, Ce, Pr, Nd, Sm, Gd, Tb, Dy, Ho, Er, Tm, Lu and Y) intermetallic compounds at 298 K.

DECLARATIONS

Author's contribution

Thermodynamic calculation and writing: Ye H, Rong M, Wang J
Data analysis and discussion: Ye H, Chen Q, Wang J
Performed literature survey and discussion: Yao Q, Rao G, Zhou H

Availability of data and materials

Supplementary Materials are available from the *Journal of Materials Informatics* or from the authors.

Financial support and sponsorship

This work was supported financially by Guangxi Natural Science Foundation (2020GXNSFFA297004), the National Natural Science Foundation of China (51971069, 51761008), Guangxi Key Laboratory of Information Materials (211007-Z) and Engineering Research Center of Electronic Information Materials and Devices (EIMD-AA202004), and Guilin University of Electronic Technology, China. The authors thank the support from the foundation for Guangxi Bagui scholars.

Conflicts of interest

All authors declared that there are no conflicts of interest.

Ethical approval and consent to participate

Not applicable.

Consent for publication

Not applicable.

REFERENCES

1. Cao XJ, Chen L, Guo S, et al. Improved thermal stability of TbF_3-coated sintered Nd-Fe-B magnets by electrophoretic deposition. *AIP Advances* 2018;8:056222. DOI
2. Buschow KHJ. Intermetallic compounds of rare-earth and 3d transition metals. *Rep Prog Phys* 1977;40:1179-256. DOI
3. Dong D, Wei G, Qian J, et al. Effects of manganese substitution on magnetic and magnetostrictive properties of $Tb_{0.5}Dy_{0.5}(Fe_{1.}x\text{-}Mnx)_{1.92}$/epoxy composites with spherical single-crystal particles. *J Rare Earths* 2022;6:1211-6. DOI
4. Cao Y, Lin K, Khmelevskyi S, et al. Ultrawide temperature range super-invar behavior of $R_2(Fe,Co)_{17}$ materials (R = rare earth). *Phys Rev Lett* 2021;127:055501. DOI PubMed
5. Huang R, Liu Y, Fan W, et al. Giant negative thermal expansion in NaZn13-type La(Fe, Si, Co)13 compounds. *J Am Chem Soc* 2013;135:11469-72. DOI PubMed
6. Cao Y, Lin K, Liu Z, et al. Role of "dumbbell" pairs of fe in spin alignments and negative thermal expansion of Lu_2Fe_{17}-based intermetallic compounds. *Inorg Chem* 2020;59:11228-32. DOI PubMed
7. Zhu H, Liu J, Wang X, Xing Y, Zhang H. Applications of terfenol-D in China. *J Alloys Compd* 1997;258:49-52. DOI
8. Nieves P, Legut D. Influence of grain morphology and orientation on saturation magnetostriction of polycrystalline Terfenol-D. *Solid State Commun* 2022;352:114825. DOI
9. Liu HF, Wang HY, Zhang Y. Research on the application status of giant magnetostrictive material in drive field. *AMM* 2015;733:249-52. DOI
10. Huiqun Y, Dong L, Huagang S. Hysteretic property of rare earth giant magnetostrictive actuator. *J Rare Earths* 2007;25:236-9. DOI
11. Yuan H, Sun H, Zhou Z. Evolvement on preparation technique of the giant magnetostrictive material. *J Mater Metall* 2003;2:115-119. Available from: http://open.oriprobe.com/articles/5829718/Evolvement_on_preparation_technique_of_the_giant_m.htm.[Last accessed on 10 Jul 2023]
12. Michels A, Weber R, Titov I, et al. Spin structures of textured and isotropic Nd-Fe-B-based nanocomposites: evidence for correlated crystallographic and spin textures. *Phys Rev Applied* 2017;7:024009. DOI
13. Yao Q, Xiong J, Liu P, et al. Determination of the phase diagrams of the $Nd_2Fe_{14}B$-$Pr_2Fe_{14}B$ isopleth. *J Alloys Compd* 2015;633:229-32. DOI
14. Fu G, Wang J, Rong MH, Rao GH, Zhou HY. Phase equilibria of the Nd-Fe-B ternary system. *J Phase Equilib Diffus* 2016;37:308-18. DOI
15. Liu W, Zhang Z, Yue M, Li Z, Zhang D, Zhang H. Effects of La substitution on the crystal structure and magnetization of MM-Fe-B alloy (MM = La, Ce, Pr, Nd). *J Magn and Magn Mater* 2018;464:61-4. DOI
16. Wang L, Wang J, Rong M, Rao G, Zhou H. Effect of wheel speed on phase formation and magnetic properties of $(Nd_{0.4}La_{0.6})$-Fe-B melt-spun ribbons. *J Rare Earths* 2018;36:1179-83. DOI
17. Chen K, Guo S, Fan XD, et al. Coercivity enhancement of (Nd,Ce)-Fe-B sintered magnets by doping Nd-Fe additives. *AIP Advances* 2017;7:025213. DOI
18. Konar B, Kim J, Jung I. Critical systematic evaluation and thermodynamic optimization of the Fe-RE system: RE = La, Ce, Pr, Nd and Sm. *J Phase Equilib Diffus* 2016;37:438-58. DOI
19. Konar B, Kim J, Jung I. Critical systematic evaluation and thermodynamic optimization of the Fe-RE system: RE = Gd, Tb, Dy, Ho, Er, Tm, Lu, and Y. *J Phase Equilib Diffus* 2017;38:509-42. DOI
20. Chen T, Wang J, Guo C, et al. Thermodynamic description of the Nd-Fe-B ternary system. *Calphad* 2019;66:101627. DOI
21. Chen T, Guo C, Li C, Du Z. Experimental investigation and thermodynamic description of the Pr-Fe-B system. *J Magn Magn Mate* 2020;497:165983. DOI
22. Li S, Rong M, Xu L, et al. Thermodynamic assessment of the RE-B (RE = Ce, Dy, Lu) binary systems. *Calphad* 2020;68:101740. DOI
23. Wei Q, Rong M, Li S, et al. Thermodynamic assessment of the RE-B (RE = Ho, Er, Tm) binary systems. *Calphad* 2020;70:101796. DOI
24. Wei Q, Rong M, Li S, et al. Thermodynamic calculation of phase equilibria of rare earth metals with boron binary systems. *Int J Mater Res* 2022;113:400-18. DOI
25. Chen T, Wang J, Rong M, Rao G, Zhou H. Experimental investigation and thermodynamic assessment of the Fe-Pr and Fe-Nd binary systems. *Calphad* 2016;55:270-80. DOI
26. Chen X, Wang J, Chen T, et al. Thermodynamic re-assessment of the Fe-Gd and Fe-Sm binary systems. *Calphad* 2017;58:151-9. DOI
27. Rong M, Chen X, Wang J, Rao G, Zhou H. Thermodynamic re-assessment of the Fe-Dy and Fe-Tb binary systems. *Calphad* 2017;59:154-63. DOI
28. Xu L, Wang J, Li S, et al. Thermodynamic re-assessment of the Fe-Tm and Fe-Ho binary systems. *Calphad* 2019;66:101646. DOI
29. Su D, Yang K, Rong M, et al. Phase transition, microstructure and solidification of Ce-La-Fe and Ce-Nd-Fe alloys: experimental investigation and thermodynamic calculation. *Calphad* 2023;80:102506. DOI
30. Richerd J. Lanthanum and cerium in pure iron. *Mem et Sci Rev Metall* 1962;59:539-548. (in French).
31. Nassau K, Cherry L, Wallace W. Intermetallic compounds between lanthanons and transition metals of the first long period: I-preparation, existence and structural studies. *J Phys Chem Solids* 1960;16:123-30. DOI

32. Haefling JF, Daane AH. Iron-lanthanum system. In: Spedding FH, Daane AH, editors. Rare Earths. New York; 1961. p. 280-281.
33. Mardani M, Fartushna I, Khvan A, Cheverikin V, Dinsdale A. Experimental investigation of phase transformations in the La-Fe and La-Fe-C systems. *Calphad* 2019;65:370-84. DOI
34. Berezutskii VV, Usenko NI, Ivanov MI. Thermochemistry of binary alloys of lanthanum with 3d-transition metals. *Powder Metall Met Ceram* 2006;45:266-71. DOI
35. Esin YO, Ermakov AF, Valishev MG, Ryss GM, Geld PV, Levin ES. Enthalpy of formation of liquid binary alloys of iron with lanthanum and cerium. *Zh Fiz Khim* 1981;55:1665-1669.
36. Vogel R. Über Cer-Eisenlegierungen. *Z Anorg Allg Chem* 1917;99:25-49. DOI
37. Gebhart JM, Etter DE, Tucker PA. Cerium-iron and cerium-nickel binary systems. In: Proceedings of the 6th Rare Earth Research Conference; United States Air Force, office of Scientific Research, Oak-Ridge National Laboratory, Gatlinburg, TN; 1967 p. 452. Available from: https://www.osti.gov/biblio/4534032. [Last accessed on 7 Jul 2023].
38. Jepson JA, Duwez P. Partial phase diagram of the iron cerium diagram. *Trans Am Soc Metals* 1955;47:543-553.
39. Buschow KHJ, van Wieringen JS. Crystal structure and magnetic properties of cerium-iron compounds. *phys stat sol (b)* 1970;42:231-9. DOI
40. Zhuang YZ, Wu CH, Shao ZB. Study of the Fe-Ce binary system. *Rare Earth* 1987;1:16-19. (in Chinese).
41. Chuang Y, Wu C, Shao Z. Investigation of the Ce Fe binary system. *J Less Common Met* 1987;136:147-53. DOI
42. Usenko N, Kotova N, Ivanov M, Berezutski V. Enthalpies of mixing in binary Fe-Sb, Ce-Fe and ternary Ce-Fe-Sb liquid alloys. *Int J Mater Res* 2016;107:13-20. DOI
43. Ivanov MI, Berezutskii VV, Shevchenko MA, Kudin VG, Sudavtsova VS. Thermodynamic properties of binary Al-Ce and Ce-Fe alloys. *Powder Metall Met Ceram* 2015;54:80-92. DOI
44. Meschel S, Nash P, Gao Q, Wang J, Du Y. The standard enthalpies of formation of some binary intermetallic compounds of lanthanide-iron systems by high temperature direct synthesis calorimetry. *J Alloys Compd* 2013;554:232-9. DOI
45. Khvan A, Mardani M, Fartushna I, Syutkin E, Cheverikin V, Dinsdale A. An experimental investigation of the thermodynamic properties of β-$Fe_{17}Ce_2$, Fe_2Ce, and ternary $Fe_{13.1\text{-}11.0}Mn_{3.9\text{-}6.0}Ce_2$ (τ1) intermetallic phases. *Thermochimica Acta* 2019;672:1-8. DOI
46. Povoden-karadeniz E, Grundy AN, Chen M, Ivas T, Gauckler LJ. Thermodynamic assessment of the La-Fe-O system. *J Phase Equilib Diffus* 2009;30:351-66. DOI
47. Su X, Tedenac J. Thermodynamic modeling of the ternary Ce-Fe-Sb system: assessment of the Ce-Sb and Ce-Fe systems. *Calphad* 2006;30:455-60. DOI
48. Ray AE. The iron-praseodymium phase diagram[R]. AFML-TR-69-239, Air Force Materials Laboratory, Wright-Paterson AFB, OH, 1969.
49. Tian JH, Huang YY, Liang JK. The Pr-Fe-B ternary system. *Sci Chin Ser A-Mathem, Phys, Astron Technol Sci* 1987;30:607-619.
50. Zhuang YH, Zhou HY, Zheng JX. Phase diagram of binary Pr-Fe system. *Acta Metall Sin* 1987;23:42-43. (in Chinese).
51. Zhang W, Li C, Su X. The Fe-Pr (Iron-Praseodymium) system. *JPE* 1999;20:158-62. DOI
52. Okamoto H. Fe-Pr (iron-praseodymium). *JPE* 1996;17:269-269. DOI
53. Ivanov M, Berezutski V, Usenko N, Kotova N. Enthalpies of mixing in liquid alloys of iron with the lanthanides. *Int J Mater Res* 2013;104:849-57. DOI
54. Gozzi D, Iervolino M, Latini A. Thermodynamics of Fe-rich intermetallics along the rare earth series. *J Chem Eng Data* 2007;52:2350-8. DOI
55. Terekhova VF, Maslova EV, Savitskiy YM. Iron-neodymium equilibrium diagram. *Russ Met* 1965;3:50-52.
56. Che GC, Liang J. Phase diagram of Nd-Fe-B ternary system. *Sci Chin Ser A-Mathem, Phys, Astron Technol Sci* 1986;29:1172-1185.
57. Schneider G, Henig E, Petzow G, Stadelmaier HH. The binary system iron - neodymium. *Int J Mater Res* 1987;78:694-6. DOI
58. Faudot F, Harmelin M, Bigot J. The iron-neodymium phase diagram. *Scripta Metallurgica* 1989;23:795-8. DOI
59. Zhang W, Liu G, Han K. The Fe-Nd (Iron-Neodymium) system. *JPE* 1992;13:645-8. DOI
60. Hennemann K, Lukas HL, Schaller H. Constitution and thermodynamics of Fe-Nd alloys/konstitution und thermodynamik von Fe - Nd-legierungen. *Int J Mater Res* 1993;84:668-74. DOI
61. Landgraf FJG, Schneider GS, Villas-boas V, Missell FP. Solidification and solid state transformations in Fe Nd: a revised phase diagram. *J Less Common Met* 1990;163:209-18. DOI
62. Okamoto H. Erratum to: Fe-Nd (iron-neodymium). *JPE* 1997;18:317-8. DOI
63. Okamoto H. Supplemental literature review of binary phase diagrams: Al-Br, B-Cd, Cd-Mg, Cd-Ti, Er-Fe, Fe-Nd, Ge-Na, Ge-Ni, Ge-Sc, Hf-W, Pb-Yb, and Re-Ti. *J Phase Equilib Diffus* 2014;35:195-207. DOI
64. Du Y, Jin ZP, Han F. Thermodynamic optimization and calculation of the Fe-Pr system. *J Chin Rare Earth Soc* 1990:p.166-170. (in Chinese).
65. Bär S, Schaller HJ. Constitution and thermodynamics of Fe-Pr alloys. *Zeitschrift fuer Metallkunde* 1995;86:388-394. Available from: https://inis.iaea.org/search/search.aspx?orig_q=RN:26070954. [Last accessed on 7 Jul 2023].
66. Zhou GJ, Zeng DC. Thermodynamic evaluation of the Fe-Pr binary system. *MSF* 2010;654-656:2442-5. DOI
67. Hallemans B, Wollants P, Roos JR. Thermodynamic assessment of the Fe-Nd-B phase diagram. *JPE* 1995;16:137-49. DOI
68. Ende M, Jung I. Critical thermodynamic evaluation and optimization of the Fe-B, Fe-Nd, B-Nd and Nd-Fe-B systems. *J Alloys Compd* 2013;548:133-54. DOI
69. Buschow K. The samarium-iron system. *J Less Common Met* 1971;25:131-4. DOI
70. Berezutskii VV, Ivanov MI. Mixing enthalpies in samarium-transition metal melts. *Powder Metall Met Ceram* 2009;48:454-61. DOI

71. Atiq S, Rawlings RD, West DRF. Phase relationships in the Fe-Co-Gd system. *J Mater Sci Lett* 1990;9:518-9. DOI
72. Atiq S, Rawlings RD, West DRF. Crystal structure of compounds $Fe_{17}Gd_2$ and $Fe_{17}Tb_2$. *J Mater Sci Technol* 1990;6:778-80. DOI
73. Atiq S, Rawlings RD, West DRF. Defects in lattices of $(Fe_{1-x}Co_x)_{17}RE_2$ compounds (RE = Gd and Tb). *J Mater Sci Technol* 1997;13:375-8. DOI
74. Novy VF, Vickery RC, Kleber EV. The gadolinium-iron system. *Trans Metall Soc AIME* 1961;221:580-585.
75. Savitskii EM, Terekhova VF, Burov IV, Chistyakov OD. Equilibrium diagram for alloys of the gadolinium-iron system. *Russ J Inorg Chem* 1961;6:883-885.
76. Copeland MI, Krrug M, Armantrout CE, Kato H. Iron-gadolinium phase diagram. US Department of the Interior, Bureau of Mines; 1962. Available from: https://books.google.com.hk/books?id=zc7GjVdaZ7IC&pg=PP1&lpg=PP1&dq=Copeland+MI,+Krrug+M,+Armantrout+CE,+Kato+H.+Iron-gadolinium+phase+diagram.+US+Department+of+the+Interior,+Bureau+of+Mines,%0D%0A1962.&source=bl&ots=pHafAj4zDs&sig=ACfU3U2mIgemCs28wqF3V62Y. [Last accessed on 7 Jul 2023].
77. Savitskii EM, Terekhova WF. Voprosy Teorii Primeneniya Redkozemelnykh Metallov. Moscow: Akademiya Nauk SSSR; 1964. p. 116-123.
78. Savitskii EM, Terekhova VF, Torchinova RS, et al. Proceedings of Conference on Rare Earth Elements; Paris: Grenoble; 1969. p. 49-60.
79. Nikolaenko IV, Nosova VV. Enthalpy of mixing of gadolinium with manganese and iron. S*ov Prog Chem* 1989;55:30-33. (in Russian) Available from: https://elibrary.ru/item.asp?id=31150749. [Last accessed on 7 Jul 2023].
80. Deodhar SS, Ficalora PJ. A study of the reaction kinetics for the formation of rare earth-transition metal laves compounds. *Metall Trans A* 1975;6:1909-14. DOI
81. Colinet C, Pasturel A, Buschow KHJ. Study of the enthalpies of formation in the Gd-(Fe, Co, Pd, Pt) systems. *Metall Trans A* 1987;18:903-7. DOI
82. Zinkevich M, Mattern N, Handstein A, Gutfleisch O. Thermodynamics of Fe-Sm, Fe-H, and H-Sm systems and its application to the hydrogen-disproportionation-desorption-recombination (HDDR) process for the system $Fe_{17}Sm_2$-H_2. *J Alloys Compd* 2002;339:118-39. DOI
83. Konar B, Kim J, Jung I. Thermodynamic modelling of Fe-Sm and Fe-Dy systems. *Can Metall Q* 2013;52:321-8. DOI
84. Liu Z, Zhang W, Sundman B. Thermodynamic assessment of the Co Fe Gd systems. *J Alloys Compd* 1995;226:33-45. DOI
85. Zinkevich M, Mattern N, Seifert HJ. Reassessment of the Fe-Gd (Iron-Gadolinum) system. *JPE* 2000;21:385-94. DOI
86. Wang W, Guo C, Li C, Du Z. A thermodynamic re-modeling of the Co-Fe-Gd system. *J Rare Earths* 2012;30:1055-63. DOI
87. Roe GJ, O'keefe TJ. The Fe-Ho binary system. *Metall Trans* 1970;1:2565-8. DOI
88. Kolesnichenko VF, Terekhova VF, Savitskii EM. Phase diagrams of thulium-iron and lutetium-iron alloys. *Metalloved Tsvetn Met Splavov Nauka* 1972;3:31-33. (in Russian).
89. Cahn RW. Binary alloy phase diagrams. *Adv Mater* 1991;3:628-9. DOI
90. Kardellass S, Servant C, Selhaoui N, Iddaoudi A. Thermodynamic evaluations of the iron-lutetium and iron-thulium systems. *Calphad* 2014;46:42-54. DOI
91. Kardellass S, Servant C, Selhaoui N, Iddaoudi A, Ait Amar M, Bouirden L. A thermodynamic assessment of the Iron+Holmium phase diagram. *J Chem Thermodyn* 2014;74:78-84. DOI
92. Dariel M, Holthuis J, Pickus M. The terbium-iron phase diagram. *J Less Common Met* 1976;45:91-101. DOI
93. Orlova IG, Eliseev AA, Chuprikov GE, Rukk F. The Fe-Tb system. *Russ J Inorg Chem* 1977;22:2557-2562.
94. Okamoto H. Fe-Tb (iron-terbium). *JPE* 1996;17:165-165. DOI
95. Chen J, Wu G, Zhao D, et al. Single-crystal growth and phase diagram of Tb_2Fe_{17} compound. *J Cryst Growth* 2001;222:779-85. DOI
96. der Goot A, Buschow K. The dysprosium-iron system: Structural and magnetic properties of dysprosium-iron compounds. *J Less Common Met* 1970;21:151-7. DOI
97. Kripyakevich PI, Frankevich DP. New compounds of rare earths with Mn and Fe, and their crystal structures. *Sov Phys Crystallogr* 1966;10:468-469. Available from: https://www.osti.gov/biblio/4562275.[Last accessed on 10 Jul 2023]
98. Strnat K, Hoffer G, Ray A. Magnetic properties of rare--Earth--Iron intermetallic compounds. *IEEE Trans Magn* 1966;2:489-93. DOI
99. Okamoto H. Dy-Fe (dysprosium-iron). *JPE* 1996;17:80-1. DOI
100. Nagai T, Shirai S, Maeda M. Thermodynamic measurement of Dy+Fe binary system by double Knudsen cell mass spectrometry. *J Chem Thermodyn* 2013;65:78-82. DOI
101. Germano D, Butera R, Gschneidner K. Heat capacity and thermodynamic functions of theRFe2 compounds (R = Gd, Tb, Dy, Ho, Er, Tm, Lu) over the temperature region 8 to 300 K. *J Solid State Chem* 1981;37:383-9. DOI
102. Meschel S, Pavlu J, Nash P. The thermochemical behavior of some binary shape memory alloys by high temperature direct synthesis calorimetry. *J Alloys Compd* 2011;509:5256-62. DOI
103. Norgren S, Hodaj F, Colinet C, Azay P. Experimental investigation on the enthalpies of formation of the $DyFe_2$, $DyFe_3$, Dy_2Fe_{17}, $ErFe_2$, and $ErFe_3$ intermetallic compounds. *Metall Mater Trans A* 1998;29:1367-74. DOI
104. Landin S, Ågren J. Thermodynamic assessment of Fe Tb and Fe Dy phase diagrams and prediction of Fe Tb Dy phase diagram. *J Alloys Compd* 1994;207-208:449-53. DOI
105. Su XP, Zhang WJ, Du ZM. Thermodynamic assessment of Fe-Dy system. *Rare Met* 1999;18:113-118. (in Chinese).
106. Buschow KHJ, van der Goot AS. Phase relations, crystal structures, and magnetic properties of erbium - iron compounds. *phys stat sol (b)* 1969;35:515-22. DOI

107. Meyer A. Erbium-iron system. *J Less Common Met* 1969;18:41-48.
108. Kolesnikov VE, Trekhova VF, Savitskii EM. Phase Diagram of the erbium-iron system. *Neorg Mater* 1971;7:495.
109. Okamoto H. Phase diagrams of binary iron alloys. OH: Materials Park, ASM International; 1993. p. 341-349. Available from: https://books.google.com.hk/books/about/Phase_Diagrams_of_Binary_Iron_Alloys.html?id=QPBUAAAAMAAJ&redir_esc=y. [Last accessed on 7 Jul 2023].
110. Zhou G, Liu Z, Zeng D, Jin Z. Thermodynamic assessment of the Fe-Er system. *Phys B Condens Matter* 2010;405:3590-3. DOI
111. Wang W, Guo C, Li C, Du Z. Thermodynamic description of the Er-Fe-Sb system. *Calphad* 2011;35:292-301. DOI
112. Wang S, Han J, Wang C, Kou S, Liu X. Thermodynamic assessment and the composition prediction of amorphous alloy in the Fe-B-Er alloy system. *J Alloys Compd* 2012;513:27-34. DOI
113. Tereshina E, Andreev A. Magnetization and specific heat study of metamagnetism in Lu_2Fe_{17}-based intermetallic compounds. *Intermetallics* 2010;18:1205-10. DOI
114. Farkas MS, Bauer AA. The solid solubility and constitution of yttrium in iron-20 to 40 w/o chromium alloys. Available from: https://www.osti.gov/biblio/4206100. [Last accessed on 7 Jul 2023].
115. Domagala RF, Rausch JJ, Levinson DW. The systems Y-Fe, Y-Ni, and Y-Cu. *Trans Am Soc Metals* 1961;53:137-155. Available from: https://www.osti.gov/biblio/4818549. [Last accessed on 7 Jul 2023].
116. Gscheidner KA. Rare earth alloys. Princeton: Van Nostrand;1961. p. 247. Available from: https://books.google.com.hk/books/about/Rare_Earth_Alloys.html?id=vj3XzwEACAAJ&redir_esc=y. [Last accessed on 7 Jul 2023].
117. von Goldbeck OK. Fe - Y Iron - Yttrium. In: IRON - Binary Phase Diagrams. Berlin: Springer Berlin Heidelberg; 1982. p. 168-70. DOI
118. Zhang BW, Liu G, Han K. The Fe-Y (iron-yttrium) system. *JPE* 1992;13:304-8. DOI
119. Hellawell A. Solid state transitions in manganese and iron solid solutions. *J Less Common Met* 1959;1:110-2. DOI
120. Buschow K. The crystal structures of the rare-earth compounds of the form R_2Ni_{17}, R_2Co_{17} and R_2Fe_{17}. *J Less Common Met* 1966;11:204-8. DOI
121. Ryss GM, Esin YO, Petrushevskii MS, Stroganov AI, Geld PV. Enthalpy of formation of iron-yttrium liquid alloys. *Zh Fiz Khim* 1976;50:771-2. Available from: https://inis.iaea.org/searchsinglerecord.aspx?recordsFor=SingleRecord&RN=10423080. [Last accessed on 7 Jul 2023].
122. Sudavtsova VS, Kurach VP, Batalin GI. Thermochemical properties of molten binary Fe--(Y, Zr, Nb, Mo) alloys. *Russ Metall* 1987.
123. Subramanian P, Smith J. Thermodynamics of formation of Y-Fe alloys. *Calphad* 1984;8:295-305. DOI
124. Dariel M, Atzmony U, Guiser R. Specific heat anomalies at the magnetic ordering temperatures of rare earth-iron laves compounds. *J Less Common Met* 1974;34:315-9. DOI
125. Mandal K, Yan A, Kerschl P, Handstein A, Gutfleisch O, Müller K. The study of magnetocaloric effect in R_2Fe_{17} (R = Y, Pr) alloys. *J Phys D Appl Phys* 2004;37:2628-31. DOI
126. Nagai T, Han W, Maeda M. Thermodynamic measurement of La-Fe and Y-Fe alloys by multi-Knudsen cell mass spectrometry. *J Alloys Compd* 2010;507:72-6. DOI
127. Du ZM, Zhang WJ, Zhuang YZ. Thermodynamic assessment of the Fe-Y system. *Rare Met* 1997;16:52-58. (in Chinese).
128. Gong W, Chen T, Li D, Liu Y. Thermodynamic investigation of Fe-Ti-Y ternary system. *Trans Nonferrous Met Soc* 2009;19:199-204. DOI
129. Lü D, Guo C, Li C, Du Z. Thermodynamic description of Fe-Y and Fe-Ni-Y Systems. *Phys Procedia* 2013;50:383-7. DOI
130. Kardellass S, Servant C, Selhaoui N, et al. Thermodynamic assessments of the Fe-Y and Ni-Sc systems. *MATEC Web Conf* 2013;3:01008. DOI
131. Kardellass S, Servant C, Selhaoui N, Iddaoudi A, Amar MA, Bouirden L. A thermodynamic assessment of the iron-yttrium system. *J Alloys Compd* 2014;583:598-606. DOI
132. Saenko I, Fabrichnaya O, Udovsky A. New thermodynamic assessment of the Fe-Y system. *J Phase Equilib Diffus* 2017;38:684-99. DOI
133. Fan L, Shen C, Hu K, Liu H, Zhang H. DFT Calculations and thermodynamic Re-assessment of the Fe-Y binary system. *J Phase Equilib Diffus* 2021;42:348-62. DOI
134. Dinsdale A. SGTE data for pure elements. *Calphad* 1991;15:317-425. DOI
135. Hillert M, Jarl M. A model for alloying in ferromagnetic metals. *Calphad* 1978;2:227-38. DOI
136. Sundman B, Jansson B, Andersson J. The Thermo-Calc databank system. *Calphad* 1985;9:153-90. DOI
137. Kim J, Jung I. Critical systematic evaluation and thermodynamic optimization of the Mn-RE system: RE = La, Ce, Pr, Nd and Sm. *J Alloys Compd* 2012;525:191-201. DOI
138. Kim J, Paliwal M, Zhou S, Choi H, Jung I. Critical systematic evaluation and thermodynamic optimization of the Mn-RE system (RE = Tb, Dy, Ho, Er, Tm and Lu) with key experiments for the Mn-Dy system. *J Phase Equilib Diffus* 2014;35:670-94. DOI
139. Ye H, Rong M, Yao Q, et al. Phase equilibria and thermodynamic properties in the RE-Ni (RE = rare earth metals) binary systems. *J Mater Sci* 2023;58:1260-92. DOI
140. The materials project. Available from: https://materialsproject.org/. [Last accessed on 19 Jun 2023].
141. The open quantum materials database. Available from: http://oqmd.org/. [Last accessed on 19 Jun 2023].
142. Du Z, Lü D. Thermodynamic modelling of the Co-Y system. *J Alloys Compd* 2004;373:171-8. DOI